X-621-64-90

TM X-55003

DETERMINATION OF THE TRIAXIALITY OF THE EARTH FROM OBSERVATIONS ON THE DRIFT OF THE SYNCOM II SATELLITE

BY

C. A. WAGNER

APRIL 1964

GODDARD SPACE FLIGHT CENTER

GREENBELT, MD.

DETERMINATION OF THE TRIAXIALITY OF THE EARTH FROM OBSERVATIONS ON THE DRIFT OF THE SYNCOM II SATELLITE

Prepared for the Communications Satellite Projects
Spacecraft Systems and Projects Division

By
C. A. Wagner

Advanced Missions and Research Division
Spacecraft Systems Branch
Spacecraft Systems and Projects Division

Goddard Space Flight Center
Greenbelt, Maryland

SUMMARY

The near-24-hour Syncom II satellite (with an almost circular orbit) has been under continuous observation by range and range-rate radar and minitrack stations for 7 months since mid-August 1963, when the orbit was relocated, placing its mean longitude at about 55 degrees west of Greenwich. During the first 4 months of this period, the satellite was allowed to drift free in the gravity fields of the earth, sun, and moon. In this first free-drift period, the satellite experienced a mean daily drift acceleration of its ascending node (with respect to Greenwich) of

$$-(1.27 \pm .02) \times 10^{-3} \text{ degrees/day}^2 . \quad (1)$$

The average growth of the semimajor axis for this period was

$$(.0993 \pm .0042) \text{ km/day} . \quad (2)$$

These values, checked by a simulated particle trajectory run on the Goddard ITEM program, confirm a significant longitude-dependent earth-gravity potential. The existence of a "triaxial earth" has been a speculation of geodesists since the early years of this century.

During the last 3 months of this 7-month drift period, starting at the end of November 1963, Syncom II was relocated at about 60 degrees west of Greenwich. In this period, the mean daily drift acceleration of the ascending node was

$$-(1.32 \pm .02) \times 10^{-3} \text{ degrees/day}^2 . \quad (3)$$

The average growth of the semimajor axis for this period was

$$(.0994 \pm .0080) \text{ km/day} . \quad (4)$$

Combining the results of (1) through (4) above for the two separate drift periods, it is estimated (on the basis of a triaxial geoid only) that the absolute magnitude of the longitude dependent-gravity coefficient J_{22} is

$$J_{22} = -(1.7 \pm .05) \times 10^{-6} .$$

This value corresponds to a difference in major and minor earth-equatorial radii of

$$(a_c - b_c) = 213 \pm 6 \text{ feet} .$$

The best present estimate of the position of the earth's major equatorial axis is

$$\lambda_{22} = 19 \pm 6 \text{ degrees west of Greenwich} .$$

In view of previous estimates of the higher order tesseral harmonics of the earth's field, the true value of J_{22}, separated from the small influence of gravity anomalies of third and higher order on the reduction for a triaxial earth only at "synchronous" altitudes, will probably be somewhat higher than the -1.7×10^{-6} reported herein. The true value of J_{22}, however, is not likely to be greater than -2.2×10^{-6} or smaller than -1.6×10^{-6}. The true location of the earth equator's major axis is not expected to differ significantly from that reported herein, when all higher tesseral harmonics are accounted for. (See Appendix B.)

The reported value of $J_{22} = -1.7 \times 10^{-6}$ implies that a maximum tangential velocity correction of

$$\Delta V_T = 5.36 \text{ ft./sec./year}$$

is required to keep a satellite with a 24-hour circular equatorial orbit continuously "on station" at a longitude midway between the longitudes of the equatorial major and minor axes of the earth. The original "conservative" Syncom I design requirement of $\Delta V_T = 17$ ft./sec./year correction capability was based on the longitude-dependent earth field of Izsak (January 1961), which is now outdated. (See Appendix B and Reference 4.)

CONTENTS

INTRODUCTION

SUMMARY OF PREVIOUS INVESTIGATIONS AND DISCUSSION OF RESULTS

The question of the existence and extent of the longitude-dependence of the earth's external gravity field has concerned geodesists since the early years of this century. (See Reference 1 for example.) The existence of a longitude-dependent field implies the existence of inhomogeneities and states of stress within the earth which are of fundamental importance to all dynamical theories of the earth's interior.

In Appendix B, I have summarized 23 reductions of gravimetric, astro-geodetic, and satellite gravity data reporting longitude-dependent terms in the earth's external gravity field represented as a series of spherical harmonics. Ten of these reductions are based on worldwide surface-gravity measurements only. Although surface measurements have the advantage of providing an excellent sampling of the field in latitude and longitude, they are seriously affected by even small uncertainties in station position with respect to the mean earth geoid, as these are of the same order-of-magnitude as the *reported* geoid deviations caused by longitude-dependent gravity.

Of the 12 satellite reduced tesseral gravity fields, those of Kozai (1962), Izsak (July 1963), Kaula (September 1963), and Guier (1963) show good general agreement in the eastern hemisphere when the constants are used as a set. All of these observers are aware, nevertheless, of the high degree of uncertainty in the reported values of the individual coefficients themselves, this uncertainty being due mainly to unresolved station-datum errors and to the limited sampling of the field from observations on a small number of medium-altitude, medium-inclination satellites.

As late as July 1963, Izsak stated (Reference 2): "It might be some time before one can arrive at definite conclusions regarding the longitude dependence of the earth's gravity field." The presence of Syncom II, high over the earth with a nearly stationary, narrow figure-8 ground track centered close to the equator, dramatically alters this gloomy outlook. The 24-hour satellite is high enough to be unaffected by the earth's atmosphere, yet is close enough to the earth to be protected from the solar wind by the "magnetosphere" of the earth, and to remain essentially unaffected by sun or moon gravity.

In theory, as the ground track is nearly stationary, any small earth-gravity anomaly in longitude will in time, cause significant drift of the ground-track configuration. In theory too, only observations of the longitude of the satellite from a single ground station are necessary to reveal this effect of the "tesseral" gravity field over an extended period of time. Long-term observations of the longitude drift of one or more 24-hour satellites should reveal the exact nature of the tesseral-gravity field to at least the third order without essential difficulty. The great height of the 24-hour satellite tends to cancel out the individual contributions to the longitudinal drift of anomalies higher than about the fourth order. It is fortunate that the initial slow westward drift of the ground track of Syncom II (August 1963 to March 1964) appears to have occurred relatively close to a point midway between the triaxial earth's major and minor equatorial axes where the perturbation of the second tesseral-gravity anomaly, for which the reduction was made, is greatest. A weighted average of the longitude-perturbation fields of Kozai (1962), Zhongolovitch (1957),

Kaula (September 1963), and Izsak (July 1963), at the altitude and longitude of Syncom II during this period, shows that the second tesseral should be contributing about 80 to 85 percent of the perturbing force. If further observations of this and other 24-hour satellites confirm this estimate, then the magnitude of the dominant J_{22} potential term, separated from higher order effects, will increase by 25 percent at most from the value reported here, which is based on the assumption that only the triaxial earth-gravity field is being measured by the drift observations. The reported location of the major equatorial axis of the triaxial earth ellipsoid is not expected to change significantly with this later refinement.

In summary, long-term observations on the drift of Syncom II have already established to a high degree of certainty that:

1. The earth must be considered to be a "triaxial ellipsoid" (for example, having a sea-level surface of this form) for the purposes of 24-hour satellite design. (For broader geodetic purposes; a significant longitude dependent gravity field exists, defining: $2.2 \times 10^{-6} < |J_{22}| < 1.6 \times 10^{-6}$; $-25^\circ < \lambda_{22} < -13^\circ$.)
2. The difference between the major and minor equatorial radii of that ellipsoid is not less than 200 feet nor greater than 225 feet.
3. The location of the major equatorial axis of the "triaxial geoid" is between 13 degrees and 25 degrees west of Greenwich.

It may be added that the study of simulated 24-hour satellite drift in a triaxial earth field, influenced also by sun and moon gravity and by sun-radiation pressure perturbations, shows that the theory of longitude drift presented in this report is substantially unaffected by all perturbations except that due to the earth's elliptical equator and possible higher order longitude-dependent earth-gravity anomalies.

1. BASIC THEORY OF THIS REDUCTION

(Determination of the Longitude Drift and Orbit Expansion for a 24-Hour Satellite With a Near-Circular Orbit Affected by a Small But Persistent Tangential Perturbing Force.)

The dominant perturbations of a 24-hour equatorial satellite in a higher order earth-gravity field have been derived many times in the literature (References 3, 4, 5, and 6). In these references, the perturbations were found by directly linearizing the equations of motion themselves and displaying the perturbed motion in appropriate geographic coordinates; no attempt was made to treat the drift of the inclined 24-hour satellite.

In this report, I will depart from this rather involved and difficult-to-visualize procedure of linearization-of-the-equations-of-motion. Instead, I will show how simple it is to derive the dominant drift and orbit-expansion equations for the 24-hour satellite by dealing with what can be called "the perturbation of the 2-body energy" of the geographically stationary satellite by the small but persistent longitude-dependent earth-gravity force. This paper will not discuss in detail the limits of validity of the expressions derived. Instead, to assess the accuracy with which these expressions predict the satellite's behavior, simulated trajectories with typical

Syncom II orbit elements have been run on Goddard's particle program "ITEM". These trajectories (Appendix A) confirm the validity of the derived drift equations to an accuracy well within the "noise levels" in the orbital elements reported for Syncom II. The equations are essentially the same as those which P. Musen has derived by a more general but more complex "energy perturbation" method (Reference 7).

In Figure 1, F is a small earth-gravity perturbation force acting tangentially to an initial circular 24-hour satellite orbit; ds is a small arc length of the satellite's path around the earth. At the beginning of the dynamics, the total energy (the sum of potential and kinetic) of the satellite in a spherical earth-gravity field (Reference 8) is

$$E = -\frac{\mu_E}{2a_s} \qquad (1)$$

where μ_E is the earth's gaussian gravity constant (3.986×10^5 km^3/sec^2). The energy added to the satellite by F per day is

$$\Delta E = \oint F ds = 2\pi a_s \bar{F} , \qquad (2)$$

where $\bar{F} = (1/2\pi) \oint F d\theta \cdot \bar{F}$, in units of force per unit mass, is the orbit averaged energy perturbing force. If the orbit is purely circular, only a tangential perturbation force can cause a change in the total energy. The ITEM simulated trajectories in Appendix A and the real Syncom II orbits both maintain eccentricities of the order of 0.0001 for periods up to 100 days. Equation (2) assumes the eccentricity is zero for the 24-hour satellite of semimajor axis a_s.

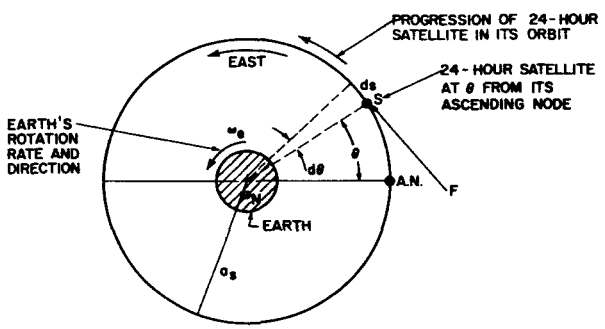

Figure 1—Orbit plane of a 24-hour satellite, looking southerly.

From (1), the change in energy of a 24-hour satellite is accompanied by a change in semimajor axis expressed by

$$\Delta E = \frac{\mu_E a_s}{2(a_s)^2} , \qquad \text{or}$$

$$\Delta a_s = \frac{2(a_s)^2 \Delta E}{\mu_E} . \qquad (3)$$

Substituting (2) into (3), the change in semimajor axis of the 24-hour near-circular orbit, per day, is approximately given by

$$\Delta a_s = \frac{4\pi (a_s)^3 \bar{F}}{\mu_E} . \tag{4}$$

From Kepler's third law, the period of a 24-hour orbit as a function of its semimajor axis is

$$T_s = \frac{2\pi (a_s)^{3/2}}{(\mu_E)^{1/2}} . \tag{5}$$

Thus, if the semimajor axis changes by Δa_s, the period change is given by

$$\Delta T_s = \frac{3\pi (a_s)^{1/2} \Delta a_s}{(\mu_E)^{1/2}} . \tag{6}$$

Substituting (4) into (6), the change in period, per day, of a 24-hour circular orbit is given by

$$\Delta T_s = \frac{12\pi^2 (a_s)^{7/2} \bar{F}}{(\mu_E)^{1/2}} . \tag{7}$$

The apparent net longitudinal drift rate of the 24-hour satellite's ground track with respect to the surface of the earth after the first sidereal day is

$$\dot{\lambda} \text{ (t = 1 sidereal day)} = - \frac{(\Delta T_s)\, 2\pi}{T_s} \text{ (radians/sidereal day)} \tag{8}$$

(See Reference 9 for example). The minus sign is taken in (8) because a gain in period is accompanied by a decrease in net geographic longitude for the initially 24-hour satellite (for example, for the daily geographic position of the ascending node). Combining Equations (7) and (5) in (8) gives

$$\dot{\lambda} \text{ (t = 1 sid. day)} = - \frac{12\pi^2 \bar{F}}{\mu_E / (a_s)^2} \text{ (rad./sid. day)} . \tag{9}$$

As the gain in semimajor axis is small over one day (and, in fact, small compared to a_s, for the entire libration period of the satellite in the triaxial earth field), the drift rate will continue to build up linearly with time initially, adding increments of (9) each day. Thus, the net longitudinal drift acceleration of an initially 24-hour satellite is

$$\ddot{\lambda} = - \frac{12\pi^2 \bar{F}}{\mu_E / (a_s)^2} \text{ (rad./sid. day}^2\text{)} . \tag{10}$$

Rewriting (4) as

$$\dot{a} = \frac{4\pi (a_s)^3 \bar{F}}{\mu_E} \quad , \text{(length units/sid. day)} \tag{11}$$

gives the expansion rate of the initially 24-hour near-circular satellite orbit due to a small but persistently acting orbit-averaged tangential perturbing force $\bar{F}$.

2. EVALUATION OF THE PERTURBING FORCE

Figure 2 shows the position of the 24-hour satellite with respect to the earth and the celestial sphere. F_r, F_ϕ and F_λ, earth-gravity perturbing forces in the radial, latitude, and longitude directions, are assumed to be acting on the satellite at s. Considering only the earth-gravity perturbation forces arising from the ellipticity of the earth's equator (Reference 10), Appendix B gives these forces as

$$F_r = \frac{\mu_E (R_0/a_s)^2}{(a_s)^2} \left\{ 9 J_{22} \cos^2 \phi \cos 2 (\lambda - \lambda_{22}) \right\} , \tag{12}$$

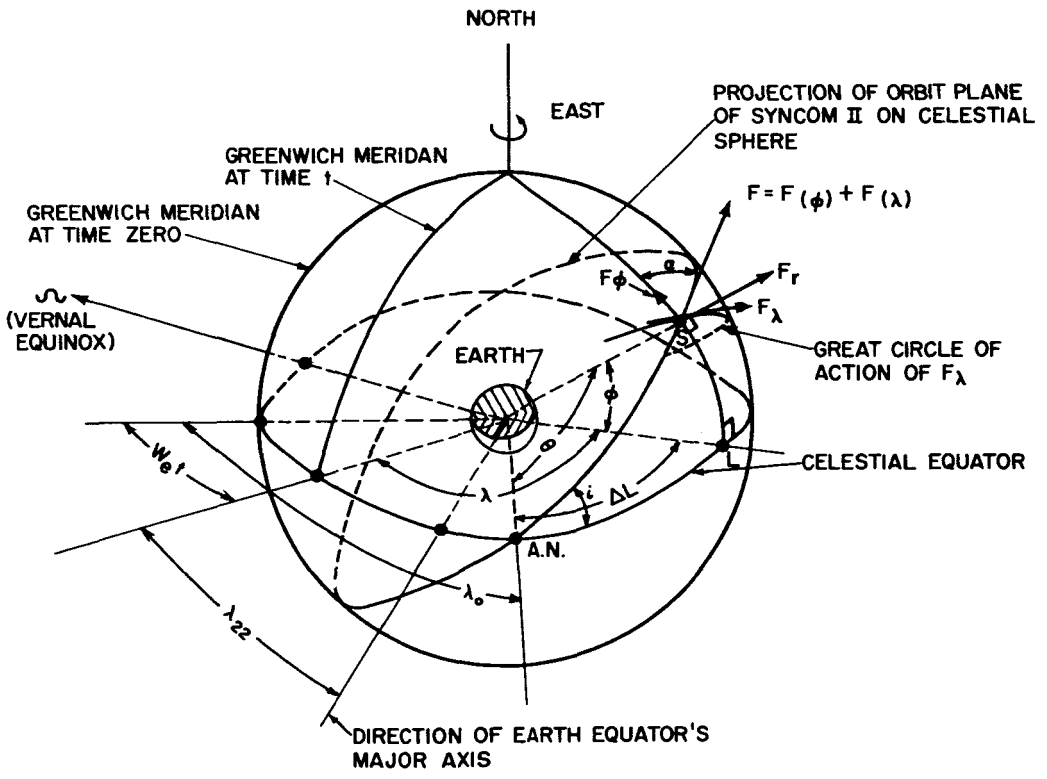

Figure 2—Position of a 24-hour satellite with a near-circular orbit with respect to the earth and the celestial sphere.

$$F_{\phi} = \frac{\mu_E (R_0/a_s)^2}{(a_s)^2} \left\{ 6J_{22} \cos\phi \sin\phi \cos 2(\lambda - \lambda_{22}) \right\}, \tag{12A}$$

$$F_{\lambda} = \frac{\mu_E (R_0/a_s)^2}{(a_s)^2} \left\{ 6J_{22} \cos\phi \sin 2(\lambda - \lambda_{22}) \right\}. \tag{13}$$

As long as the orbit is nearly circular, F_r will have negligible contribution to F. The contribution to F from F_{ϕ} is:

$$F_{(\phi)} = F_{\phi} \cos\alpha = K \sin\phi \cos\phi \cos\alpha \cos 2(\lambda - \lambda_{22}) \tag{14}$$

K is a constant for a single orbit.

$$K = 6J_{22} \left(\frac{\mu_E R_0^2}{(a_s)^4} \right). \tag{14A}$$

In the right spherical triangle AN, s, L, note the following trigonometric relations:

$$\cos(i) = \frac{\tan\Delta L}{\tan\theta}, \tag{15A}$$

$$\cos\alpha = \frac{\tan\phi}{\tan\theta}, \tag{15B}$$

$$\sin\phi = \sin(i) \sin\theta, \tag{15C}$$

$$\sin\alpha = \frac{\cos(i)}{\cos\phi}. \tag{15D}$$

From (15A),

$$\Delta L = \tan^{-1} \left[\tan\theta \cos(i) \right]. \tag{16}$$

Let the geographic longitude of the satellite at the ascending node (AN) be λ_0. Counting time from this orbital position, the geographic longitude of the 24-hour satellite at s in its near-circular orbit is

$$\lambda = \lambda_0 + \Delta L - \omega_{et} \quad \text{(Figure 2)}$$

or, using (16),

$$\lambda = \lambda_0 + \tan^{-1} \left[\tan\theta \cos(i) \right] - \omega_{et}. \tag{17}$$

w_e is the earth's sidereal rotation rate. For the 24-hour satellite (starting the dynamics with S. at A.N., for convenience), $\theta \doteq w_e t$, so that (17) becomes

$$\lambda = \lambda_0 + \tan^{-1}\left[\tan\theta\cos(i)\right] - \theta \ , \tag{18}$$

approximately. The function $\tan^{-1}\left[\tan\theta\cos(i)\right] - \theta$ is even about $\theta = 0$ and $\theta = \pi/2$, with a period of π, and behaves like a somewhat distorted sine function (Figure 3 and Appendix C). Call this function $\Delta\lambda$ and note that for $i < 33$ degrees, $\Delta\lambda$ is always less than 5°. Thus, using (18) and assuming i is sufficiently small ($i < 45°$ proves to be a sufficient restriction on the inclination), $\cos 2(\lambda - \lambda_{22})$ for the 24-hour satellite can be approximated by

$$\cos 2(\lambda - \lambda_{22}) \doteq \cos 2(\lambda_0 - \lambda_{22}) - 2\Delta\lambda \sin 2(\lambda_0 - \lambda_{22}) = -\cos 2\gamma_0 + 2\Delta\lambda \sin 2\gamma_0 \ . \tag{18A}$$

Similarly, $\sin 2(\lambda - \lambda_{22})$ can be approximated by

$$\sin 2(\lambda_0 - \lambda_{22}) + 2\Delta\lambda \cos 2(\lambda_0 - \lambda_{22}) = -\sin 2\gamma_0 - 2\Delta\lambda \cos 2\gamma_0 \doteq \sin 2(\lambda - \lambda_{22}) \tag{18B}$$

In Figure 3, γ_0 is the geographic longitude of the node of the 24-hour nearly circular satellite orbit with respect to the minor equatorial axis. With these expansions [(18A) and (18B)], and using (15B), (14) becomes

$$F_{(\phi)} = K \frac{\sin\phi\cos\phi\tan\phi}{\tan\theta}\left\{-\cos 2\gamma_0 + 2\Delta\lambda \sin 2\gamma_0\right\} \ .$$

Using (15C) in the above expression, the contribution to the perturbing force F due to F_ϕ becomes

$$F_{(\phi)} = K \frac{\sin^2(i)\sin 2\theta}{2}\left\{-\cos 2\gamma_0 + 2\Delta\lambda \sin 2\gamma_0\right\} \ . \tag{19}$$

Writing $\Delta\lambda \doteq \Delta\lambda\,(\max)\sin 2\theta$, (19) becomes

$$F_{(\phi)} \doteq K\sin^2(i)\left[-\cos 2\gamma_0\right]\frac{\sin 2\theta}{2} - K\sin^2(i)\,\Delta\lambda\,(\max)\left[\sin 2\gamma_0 \sin^2 2\theta\right] \tag{20}$$

Averaging $F_{(\phi)}$ over $0 \le \theta \le 2\pi$, (20) gives

$$\bar{F}_{(\phi)} = \frac{1}{2\pi}\int_0^{2\pi} F_{(\phi)}\, d\theta = -\frac{\sin^2 i\Delta\lambda\,(\max)}{2}\left[K\sin 2\gamma_0\right] \tag{21}$$

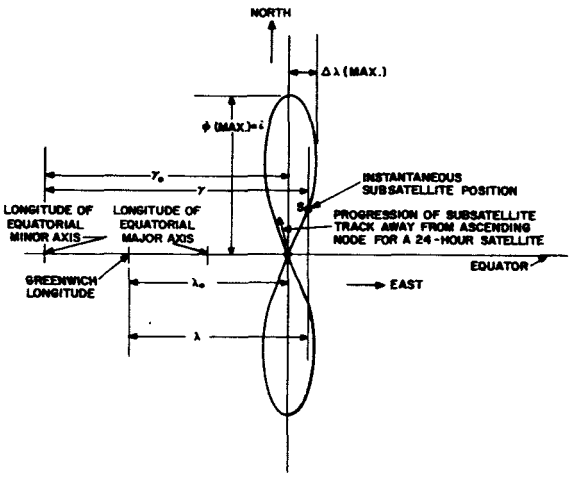

Figure 3—Geographic subsatellite track of 24-hour satellite in a near-circular orbit.

The contribution to F from F_λ is

$$F_{(\lambda)} \approx F_\lambda \cos(90 - \alpha) = F_\lambda \sin\alpha = K \sin\alpha \cos\phi \left\{ - \sin 2\gamma_0 - 2\Delta\lambda \cos 2\gamma_0 \right\} , \tag{22}$$

from (13) and (18B). Using (15D) in (22), and noting that $\Delta\lambda \doteq \Delta\lambda\,(\max) \sin 2\theta$, as before, gives the contribution to F from F_λ as

$$F_{(\lambda)} = K \cos(i) \left\{ - \sin 2\gamma_0 - 2\Delta\lambda\,(\max) \sin 2\theta \cos 2\gamma_0 \right\} . \tag{23}$$

Averaging $F_{(\lambda)}$ over $0 \le \theta \le 2\pi$, (23) gives

$$\bar{F}_{(\lambda)} = - K \cos(i) \sin 2\gamma_0 . \tag{24}$$

Thus, combining the contributions of the latitude and longitude perturbations to the average perturbation force over a single 24-hour orbit, (21) and (24) sum to produce

$$\bar{F}\,(\text{total}) = \bar{F}_{(\phi)} + \bar{F}_{(\lambda)} = - K \sin 2\gamma_0 \left\{ \cos(i) + \frac{\sin^2(i)\,\Delta\lambda\,(\max)}{2} \right\} . \tag{25}$$

3. COMPLETION OF THE DERIVATION OF THE DRIFT EQUATIONS

Appendix C shows that

$$\Delta\lambda\,(\max) = \tan^{-1}\left[\sec(i)\right] - 45^\circ .$$

It is also shown there that, to a high degree of accuracy for $i < 50^\circ$,

$$\cos(i) + \frac{\sin^2 \Delta\lambda\,(\max)}{2} \doteq \frac{1 + \cos^2(i)}{2} .$$

Numerically integrated orbits have shown that the drift theory for a 24-hour satellite stemming from (25) is in error by more than 2 percent for $i > 45^\circ$. With this restriction on orbit inclination, using the above approximation for the inclination factor, we can rewrite the longitude drift and orbit expansion equations (10) and (11), evaluating $\bar{F}$ by (25), giving

$$\ddot{\gamma} = \frac{12\pi^2 K}{\mu_E / (a_s)^2} \left[\frac{\cos^2(i) + 1}{2} \right] \sin 2\gamma_0 , \text{ (rad./sid. day}^2\text{)} \tag{26}$$

$$\dot{a} = - \frac{4\pi\,(a_s)^3 K}{\mu_E} \left[\frac{\cos^2(i) + 1}{2} \right] \sin 2\gamma_0 , \text{ (length units/sid. day)} . \tag{27}$$

Substituting (14A) into (26) and (27) reduces these expressions to

$$\ddot{\gamma} = 72\pi^2 J_{22} (R_0/a_s)^2 \left[\frac{\cos^2(i)+1}{2}\right] \sin 2\gamma_0 \quad , \text{(rad./sid. day}^2\text{)} \tag{28}$$

$$\dot{a} = -24\pi J_{22} (R_0/a_s) R_0 \left[\frac{\cos^2(i)+1}{2}\right] \sin 2\gamma_0, \text{ (length units/sid. day).} \tag{29}$$

Define a nondimensional change of semimajor axis from a_s during the drift as

$$a_1 = \frac{a - a_s}{a_s} = \frac{\Delta a}{a_s} \text{ ; so that, } \dot{a}_1 = \frac{\dot{a}}{a_s} . \tag{29A}$$

With (29A), (29) becomes

$$\dot{a}_1 = -24\pi J_{22} (R_0/a_s)^2 \left\{\frac{\cos^2(i)+1}{2}\right\} \sin 2\gamma_0 \quad , \text{(1/sid. day)}. \tag{30}$$

Define:

$$A_{22} = -72\pi^2 J_{22} (R_0/a_s)^2 \left\{\frac{\cos^2(i)+1}{2}\right\} \quad , \text{(rad./sid. day}^2\text{)}. \tag{30A}$$

With (30A), (28) and (30) become;

$$\ddot{\gamma} + A_{22} \sin 2\gamma_0 = 0 \quad , \text{(rad./sid. day}^2\text{)} \tag{31}$$

$$\dot{a}_1 - \frac{A_{22} \sin 2\gamma_0}{3\pi} = 0 \quad , \text{(1/sid. day)}. \tag{32}$$

Note that π in (32) has dimensions of rad./sid. day. It must be understood that (31) describes the *net* daily geographic acceleration of the initially 24-hour satellite with respect to the earth's minor equatorial axis. Stated another way, (31) describes the geographic drift of the entire originally stationary, figure-8 ground track (Figure 3). Similarly, (32) describes the net daily orbit-expansion rate of the 24-hour satellite. In particular, it is convenient to treat the motion of the ascending node of the orbit in geographic longitude as a reference for the entire configuration. In what follows, therefore, γ will refer always to the geographic longitude of the ascending node east of the equatorial minor axis; γ_0 will refer to the initial geographic longitude of the A.N. east of the minor axis, at the start of the dynamics under consideration. (31) and (32) can thus be re-written in terms of the general nodal longitude position γ, to give the relevant partially uncoupled long-term drift and orbit-expansion differential equations for the near-24-hour near-circular orbit satellite:

$$\ddot{\gamma} + A_{22} \sin 2\gamma = 0 \quad , \text{(rad./sid. day}^2\text{)} \tag{33}$$

$$\dot{a}_1 - \frac{A_{22} \sin 2\gamma}{3\pi} = 0 \quad , (1/\text{sid. day}). \tag{34}$$

4. GENERAL CONSIDERATIONS OF THE SOLUTIONS OF THE DRIFT EQUATIONS

Equation (33) can be integrated directly for the geographic drift rate by noting that

$$\ddot{\gamma} = \frac{d\dot{\gamma}}{dt} = \frac{d(\dot{\gamma})^2}{2\dot{\gamma}\, dt} = \frac{d(\dot{\gamma})^2}{2d\gamma} .$$

Thus (33) can be separated to

$$d(\dot{\gamma})^2 = -2A_{22} \sin 2\gamma \, d\gamma . \tag{35}$$

Since the variables $(\dot{\gamma})^2$ and γ are separated in (35), (35) integrates to

$$(\dot{\gamma})^2 = A_{22} \cos 2\gamma + C_1 . \tag{36}$$

With the initial condition that $\dot{\gamma} = \dot{\gamma}_0$ at $\gamma = \gamma_0$, (36) becomes

$$\dot{\gamma} = \left[(\dot{\gamma}_0)^2 + A_{22} \left(\cos 2\gamma - \cos 2\gamma_0\right)\right]^{1/2} , \tag{37}$$

giving the drift rate of the 24-hour satellite as a function of the initial drift rate $\dot{\gamma}_0$, the earth-gravity constant A_{22}, the initial longitude east of the minor axis γ_0, and the instantaneous longitude γ. Returning to the semicoupled system of equations (33) and (34), the explicit dependence of the equations on the location from the minor axis and the magnitude of the equatorial ellipticity may be eliminated by multiplying (33) by $1/3\pi$ and adding the resulting equation to (34), giving

$$\ddot{\gamma} + 3\pi \dot{a}_1 = 0 , \tag{38}$$

(38) can be rewritten as

$$\frac{d(\dot{\gamma})}{dt} + 3\pi \dot{a}_1 = 0 = d(\dot{\gamma}) + 3\pi \dot{a}_1 \, dt = d(\dot{\gamma}) + 3\pi \, d(a_1) . \tag{39}$$

Separation of the variables $\dot{\gamma}$ and a_1 is thus achieved in (39). (39) integrates directly to

$$3\pi a_1 + \dot{\gamma} = C_2 . \tag{40}$$

With the initial conditions: $a_1 = 0$, when $\dot{\gamma} = 0$ (the satellite is in the momentarily stationary ground-track configuration); $C_2 = 0$. If γ_0 in (37) is also the longitude of this initially stationary

orbit, $(\dot{\gamma}_0)^2 = 0$ there, and (37) in (40) yields for a_1, the semimajor axis change from "synchronism" in the drift motion,

$$a_1 = \pm \frac{(A_{22})^{1/2} (\cos 2\gamma - \cos 2\gamma_0)^{1/2}}{3\pi} , \tag{41}$$

(41) shows explicitly that the semimajor axis is bounded in long-term drift from a stationary orbit. From (33), since $A_{22} > 0$, if $0 < \gamma_0 < 90°$, drift proceeds *towards* the nearest longitude of the earth's equatorial minor axis (in a $-\gamma$ direction). If $-90° < \gamma_0 < 0°$, (33) shows that drift again proceeds *toward* the nearest minor axis longitude (in a $+\gamma$ direction). Thus, in all cases of drift from a stationary geographic configuration, $\cos 2\gamma - \cos 2\gamma_0$ is a positive function which has a maximum when $\gamma = 0$ (when the satellite has drifted over the longitude of the minor axis). Thus (41) gives (for the librations of a 24-hour satellite)

$$a_1 \text{ (max)} = \left| \frac{(A_{22})^{1/2} (1 - \cos 2\gamma_0)^{1/2}}{3\pi} \right| . \tag{42}$$

Again it is noted that π in (42) has units of rad/sid. day. An absolute maximum semimajor axis change in the drift occurs when the "synchronous" condition is established near the longitude of the major equatorial axis. Here, $\gamma_0 = -90°$, $\cos 2\gamma_0 = -1$, and

$$a_1 \text{ (absolute maximum for a librating 24-hour satellite)} = \frac{(2A_{22})^{1/2}}{3\pi} \tag{43}$$

For the constant $J_{22} = -1.7 \times 10^{-6}$ (derived in this study from long-term observations on the drift of the Syncom II satellite) and using the additional constants from this study: $i = 33°$, $a_s \doteq 42166$ km, $R_0 = 6368.388$ km; (30A) gives

$$A_{22} = 23.2 \times 10^{-6} \text{ (rad./sid. day}^2\text{)} .$$

(43) then gives

a_1 (absolute max.) $= .72 \times 10^{-3}$, from which, by (29A),

Δa (absolute max. from a "synchronous" condition near the equatorial major axis, for a satellite of $i = 33°$) $= 30.7$ km .

Thus the assumption made in (10) and (11), to approximate the slightly varying semimajor axis by a_s (a constant) throughout the drift motion, appears amply justified.

Figure 4 is a graph of (41) for a_1 vs. γ (the longitude with respect to the nearest minor axis location) as a function of γ_0, the longitude in the initially stationary configuration.

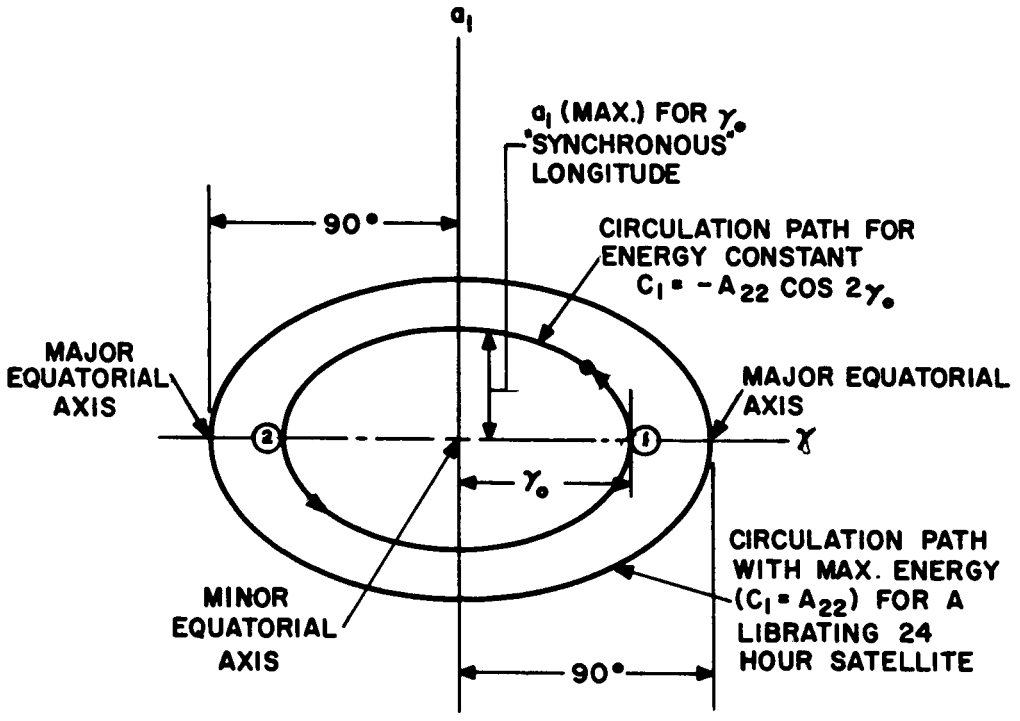

Figure 4—Libration with longitude of the semimajor axis of a 24-hour satellite as a function of the longitude of the initially stationary configuration.

Note that (41) allows equal ± values for a_1 for each γ. Suppose the satellite is initially at $+\gamma_0$ (position 1 in Figure 4) from the nearest location of the minor axis: From (33), $\sin 2\gamma_0$ being positive, the satellite begins to drift west (attaining a negative drift rate) towards the minor axis. But, from (40), since $C_2 = 0$, $a_1 = -(\dot{\gamma})/3\pi > 0$; the drift therefore proceeds counterclockwise in Figure 4, around the central point of the minor axis and $a_1 = 0$, along the upper portion of the two-valued arc determined from (41).

The same situation holds for the motion beginning or stemming away from the "synchronous" longitude at $-\gamma_0$, position 2 in Figure 4. Here $\sin 2\gamma_0$ is negative, and the drift proceeds at a positive rate to the east. Again from (40), as soon as the satellite leaves position 2, $a_1 = -(\dot{\gamma})/3\pi < 0$, and the circulation continues in a counterclockwise direction. Every trajectory in the phase plane $a_1 \Leftrightarrow \gamma$ may be conveniently defined by the constant C_1 of the "energy integral" of the drift motion (36). Since (33) is the equation-of-motion defining the large-angle oscillations of a mathematical pendulum (in the case of the 24-hour-orbit satellite, the point of symmetry is the minor axis where $2\gamma = 0$), it can be expected that the general solutions in that theory apply to the long-term librations of the "synchronous satellite" (Appendix D). For example, in (36), with a momentarily "synchronous" condition at γ_0 being given by $\dot{\gamma}_0 = 0$, the "energy constant" is evaluated as

$$C_1 = -A_{22} \cos 2\gamma_0 .$$

With this evaluation, (36) becomes

$$(\dot{\gamma})^2 - A_{22} \cos 2\gamma = - A_{22} \cos 2\gamma_0 \ . \tag{44}$$

Solving for the initially "synchronous" longitude as a function of any longitude in the drift and the corresponding longitude rate, (44) gives

$$\gamma_0 = \frac{1}{2} \cos^{-1} \left[\cos 2\gamma - \frac{(\dot{\gamma})^2}{A_{22}} \right] . \tag{45}$$

Since $(\dot{\gamma})^2/A_{22} \geq 0$, the argument of $\cos^{-1}$ in (45) is always less than or equal to 1. Thus, as long as $\cos 2\gamma - (\dot{\gamma})^2/A_{22} \geq -1$, (45) will give a real solution for the momentarily "synchronous" longitude with respect to the minor axis. But, if $\cos 2\gamma - (\dot{\gamma})^2/A_{22} < -1$, there will be no real momentarily "synchronous" configuration for the near-24-hour satellite. With this energy, the world-circulation regime commences, corresponding to the over-the-top, high-energy regime of the mathematical pendulum (Reference 3). The above inequality implies that, for the commencement of "world circulation" for the near-24-hour satellite,

$$(\dot{\gamma})^2 \geq A_{22} (1 + \cos 2\gamma), \text{ or}$$

$$(\dot{\gamma})^2 \geq 2 A_{22} \cos^2 \gamma \ . \tag{46}$$

When $2\gamma = 0$, or the satellite is over the minor axis, (46) allows the maximum possible drift rate for a librating 24-hour satellite:

$$\dot{\gamma}(\max)_{\text{for libration}} = \left(2A_{22}\right)^{1/2} , \text{ (rad./sid. day)} . \tag{47}$$

For example, using the reported value of $A_{22} = 23.2 \times 10^{-6}$ rad./sid. day^2 for the inclination of the Syncom II satellite, (47) gives

$$\dot{\gamma}(\max)_{\text{for libration with } J_{22} = -1.7 \times 10^{-6},\ i = 33^\circ} = (46.4 \times 10^{-6})^{1/2} = .39 \text{ degrees/day.} \tag{48}$$

5. APPROXIMATIONS TO THE EXACT DRIFT SOLUTIONS FOR PERIODS VERY CLOSE TO SYNCHRONOUS

Expanding the drift from the "synchronous" longitude ($\gamma = \gamma_0$ in this section) in a Taylor series, with respect to increments of time Δt from the momentarily stationary condition,

$$\gamma(\Delta t) = \gamma_0 + \dot{\gamma}_0 \Delta t + \ddot{\gamma}_0 \frac{(\Delta t)^2}{2} + \dddot{\gamma}_0 \frac{(\Delta t)^3}{6} + \gamma_0^{[4]} \frac{(\Delta t)^4}{24}$$

$$+ \gamma_0^{[5]} \frac{(\Delta t)^5}{120} + \gamma_0^{[6]} \frac{(\Delta t)^6}{720} + \gamma_0^{[7]} \frac{(\Delta t)^7}{5040} + \gamma_0^{[8]} \frac{(\Delta t)^8}{40320} + \cdots \tag{50}$$

Differentiating (33) six times with respect to time, it is clear that all derivatives in (50) can be written as functions of A_{22}, γ_0 and $\dot{\gamma}_0$. Noting that $\gamma(\Delta t) - \gamma_0 = \Delta\lambda$ (the geographic longitude with respect to the "synchronous" configuration) and $\dot{\gamma}_0 = 0$, (50) can be shown to reduce to the expansion

$$\Delta\lambda = \left(-A_{22} \sin 2\gamma_0\right) \frac{(\Delta t)^2}{2} + \left[\left(A_{22}\right)^2 \sin 4\gamma_0\right] \frac{(\Delta t)^4}{24} + \left[\left(A_{22}\right)^3 \sin 2\gamma_0 \left(4 \sin^2 2\gamma_0 - 1\right)\right] \frac{(\Delta t)^6}{180}$$

$$- \left[\left(A_{22}\right)^4 \sin 4\gamma_0 \left(34 \sin^2 2\gamma_0 - 1\right)\right] \frac{(\Delta t)^8}{10080} + \cdots \quad (51)$$

It is apparent that, as $\Delta t \to 0$, the higher order terms of (51) become increasingly more insignificant to the total drift, in comparison to the terms of lower order.

In Appendix D, the exact "elliptic integral" of motion from (33) is calculated from a synchronous longitude of 60° east of the minor axis. This calculation demonstrates that the simple term-inclusion-time criterion below gives an adequately converging series to the "exact" drift. In the actual reduction, all higher order terms in (51) which are less in magnitude than the root mean square (rms) error of the observed Syncom II longitudes, are ignored. Section 7 of this report shows that this rms error of longitude determination for the ascending equator crossings of Syncom II from August 1963 to March 1964 has been of the order of ±.025 degrees. Thus, 0.025° is used below in forming the minimum-time-term-inclusion criterion for each term of (51). A_{22} is assumed to be 23.2×10^{-6} rad./sid. day^2.

A) For inclusion of the $(\Delta t)^4$ term:

$|\sin 4\gamma_0|$ is maximum when $\gamma_0 = \pm 22.5°$ and $\pm 67.5°$.

Therefore,

$$\left|\Delta\lambda_{max} \text{ (from the fourth-order term)}\right| = \left(A_{22}\right)^2 \frac{(\Delta t)^4}{24} . \quad (52A)$$

Solving (52A) for Δt, when $\left|\Delta\lambda_{max} \text{ (4th order)}\right| = .025°$,

$$\Delta t \text{ (min. fourth-order term inclusion)} = \left(.025 \times 24/57.3 \times \left[23.2 \times 10^{-6}\right]^2\right)^{1/4}$$

$$= 66.5 \text{ sid. days from "synchronism"} .$$

B) For inclusion of the $(\Delta t)^6$ term:

$\left|\sin 2\gamma_0 \left(4 \sin^2 2\gamma_0 - 1\right)\right|$ is maximum when $\gamma_0 = \pm 45°$.

Therefore,

$$\left|\Delta\lambda_{max} \text{ (from the sixth-order term)}\right| = \left(A_{22}\right)^3 \frac{(\Delta t)^6}{60} . \quad (52B)$$

Solving (52B) for Δt, when $|\Delta\lambda_{max}$ (sixth order)$|$ = .025°,

Δt (min. for sixth-order term inclusion) = $\left(.025 \times 60/57.3 \times \left[23.2 \times 10^{-6}\right]^3\right)^{1/6}$

= 113. sid. days from "synchronism" .

C) For inclusion of the $(\Delta t)^8$ term:

$|\sin^4 \gamma_0 \left(34 \sin^2 2\gamma_0 - 1\right)|$ is maximum when $\gamma_0 = \pm 59\,1/4°$.

Therefore,

$$|\Delta\lambda_{max} \text{ (from the eighth-order term)}| = 21.2 \left(A_{22}\right)^4 \frac{(\Delta t)^8}{10080} \tag{52C}$$

Solving (52C) for Δt, when $|\Delta\lambda_{max}$ (eighth order)$|$ = .025°,

Δt (min. for eighth-order term inclusion) = $\left(10080 \times .025/21.2 \times 57.3 \times \left[23.2 \times 10^{-6}\right]^4\right)^{1/8}$

= 171. sid. days from "synchronism" .

Similarly, expanding $a_1(t)$ in a Taylor series about the time of "synchronism", (t_0, γ_0):

$$a_1\left(t_0 + \Delta t\right) = \left(a_1\right)_0 + \left(\dot{a}_1\right)_0 (\Delta t) + \left(\ddot{a}_1\right)_0 \frac{(\Delta t)^2}{2} + \left(\dddot{a}_1\right)_0 \frac{(\Delta t)^3}{6} + \cdots . \tag{53}$$

But, from (34),

$$\left(\dot{a}_1\right)_0 = \frac{A_{22} \sin 2\gamma_0}{3\pi} . \tag{53A}$$

Differentiating (53A) with respect to time,

$$\left(\ddot{a}_1\right)_0 = \frac{2\dot{\gamma}_0 A_{22} \cos 2\gamma_0}{3\pi} = 0 , \tag{53B}$$

since $\dot{\gamma}_0 = 0$. Differentiating (53B) with respect to time,

$$\left(\dddot{a}_1\right)_0 = \frac{-4\left(\dot{\gamma}_0\right)^2 A_{22} \sin 2\gamma_0}{3\pi} + \frac{2\ddot{\gamma}_0 A_{22} \cos 2\gamma_0}{3\pi} = \frac{-\left(A_{22}\right)^2 \sin 4\gamma_0}{3\pi} , \tag{54}$$

using equation (33). From the conventional definition of a_1, $\left(a_1\right)_0 = 0$. (53) then becomes

$$a_1 \text{ (at } \Delta t \text{ from "synchronism")} = \frac{\left(A_{22} \sin 2\gamma_0\right)\Delta t}{3\pi} - \frac{\left(A_{22}\right)^2 \sin 4\gamma_0 (\Delta t)^3}{18\pi} + \cdots , \tag{54A}$$

with the results of (53A), (53B), and (54) in (53).

Section 7 shows that the rms error of semimajor axis determination for Syncom II (including sun and moon "noise") is of the order of ±0.5 km. Therefore, the rms error to be expected in a_1 is of the order of .5/42166. = 1.185×10^{-5}. Following the procedure for the longitude drift, 1.185×10^{-5} is used below to determine the minimum time for the inclusion of the terms beyond the first on the righthand side of (54A), to ensure adequate convergence of the infinite series for $a_1(\Delta t)$.

A) For inclusion of the $(\Delta t)^3$ term:

$$|\sin 4\gamma_0| \text{ is maximum when } \gamma_0 = \pm 22.5^\circ \text{ and } \pm 67.5^\circ .$$

Therefore,

$$\left| a_{1(max)} \quad [\text{from the third-order term of (54A)}] \right| = \frac{(A_{22})^2 (\Delta t)^3}{18\pi} . \tag{55}$$

Solving (55) for Δt, when $|a_1(max)| = 1.185 \times 10^{-5}$,

$$\Delta t \ [\text{min. for the third-order term inclusion in (54A)}] = \left[\frac{1.185 \times 10^{-5} \times 18\pi}{23.2 \times 10^{-12}} \right]^{1/3}$$

$$= 108 \text{ sid. days from synchronism .}$$

From a "synchronous" configuration at 54.8° west of Greenwich, on or about 6 September 1963, Syncom II drifted to 59.2° west of Greenwich on 28 November 1963, where it was "stopped" by the tangential firing of on-board cold-gas jets. A second free-drift period followed from a "synchronous" configuration at 59.2° west on about 29 November 1963, to 66.3° west on 18 March 1964, where the on-board tangential jets were fired to speed up the westward drift. Of the 34 separate orbits calculated by the Goddard Data and Tracking Systems Directorate for these free-drift periods, only 7 fell outside the minimum 66-day period around a condition of "synchronism", for which the inclusion of higher order terms in (54A) would be necessary in reducing the drift data according to that theory. The data reduction of Section 7 includes only those orbits falling within the minimum 66-day period around "synchronism". Further refinement of this reduction to include the 7 outside-of-synchronous orbits (according to the criterion of this chapter), will be made in the near future. This refinement is not expected to materially affect the results of this report.

6. DETERMINATION OF EARTH-EQUATORIAL ELLIPTICITY FROM TWO OBSERVATIONS OF DRIFT ACCELERATION AT A GIVEN LONGITUDE SEPARATION

Given two independent near-synchronous drifts (in the sense discussed previously), whose momentarily synchronous longitudes $(\gamma_0)_1$ and $(\gamma_0)_2$ are separated by $\nabla\lambda$. Let the two drift accelerations at these two "synchronous" configurations be $(\ddot{\gamma}_0)_1$ and $(\ddot{\gamma}_0)_2$. The drift accelerations may be determined from drift-data reduction according to the theory of (51).

From (33),

$$(\ddot{\gamma}_0)_1 = -(A_{22})_1 \sin 2(\gamma_0)_1 \tag{56}$$

$$(\ddot{\gamma}_0)_2 = -(A_{22})_2 \sin 2\left[(\gamma_0)_1 + \nabla\lambda\right] , \tag{57}$$

since $(\gamma_0)_2 - (\gamma_0)_1 = \Delta\lambda = (\lambda_0)_2 - (\lambda_0)_1$. Expanding (57) and dividing by (56) gives

$$\left[\frac{(\ddot{\gamma}_0)_2}{(\ddot{\gamma}_0)_1}\right]\left[\frac{(A_{22})_1}{(A_{22})_2}\right] = \cos 2\nabla\lambda + \sin 2\nabla\lambda \cot 2(\gamma_0)_1 . \tag{58}$$

Solving (58) for $(\gamma_0)_1$,

$$(\gamma_0)_1 = \frac{1}{2}\tan^{-1}\left\{\frac{\sin(\nabla\lambda)}{\frac{(\ddot{\gamma}_0)_2 (A_{22})_1}{(\ddot{\gamma}_0)_1 (A_{22})_2} - \cos 2(\nabla\lambda)}\right\} . \tag{59}$$

The quadrant of $(\gamma_0)_1$ is either the first or the fourth, because drift acceleration is always in the direction of the *nearest* longitude extension of the earth's minor equatorial axis. Once the minor axis is located by (59), the absolute value of J_{22} in the earth's triaxial gravity field can be determined through (56) and (30A), for example, as

$$J_{22} = \frac{(A_{22})_1}{72\pi^2\left[R_0/(a_s)_1\right]^2\left[\frac{\cos^2(i)_1 + 1}{2}\right]} = \frac{(\ddot{\gamma}_0)_1}{72\pi^2 \sin 2(\gamma_0)_1 \left[R_0/(a_s)_1\right]^2 \left[\frac{\cos^2(i)_1 + 1}{2}\right]} . \tag{60}$$

Note that the units of $(\ddot{\gamma}_0)_1$ in (60) must be those of radians/sidereal day^2 so that J_{22} will be dimensionless. Note also that in (59), using the result of (30A),

$$\frac{(A_{22})_1}{(A_{22})_2} = \left[\frac{(a_s)_2}{(a_s)_1}\right]^2 \left[\frac{\cos^2(i)_1 + 1}{\cos^2(i)_2 + 1}\right] \tag{61}$$

Using (59), since $(\lambda_0)_1$ is known from the data reduction (the geographic longitude of the "synchronous" configuration), the geographic longitude of the nearest minor axis location can be calculated as

$$\gamma_{22} = (\lambda_0)_1 - (\gamma_0)_1 . \tag{61A}$$

Similarly, the geographic longitude of the nearest major equatorial axis location can be calculated from

$$\lambda_{22} = (\lambda_0)_1 - (\gamma_0)_1 + 90^\circ . \tag{61B}$$

(See figure 3).

Following the theory of Reference 10, the difference in major and minor equatorial radii of the earth's triaxial geoid $(a_0 - b_0)$, is related to the gravity constant J_{22} by

$$a_0 - b_0 = -6R_0 J_{22} . \tag{62}$$

7. REDUCTION OF 27 SYNCOM II ORBITS TO DETERMINE THE EARTH'S EQUATORIAL ELLIPTICITY

Appendix A tabulates the 27 Syncom II orbits from which the reduction below was made. Table 1 gives the estimated ascending equator crossings nearest to the epoch of these orbits. These were calculated by hand, and therefore are listed only to 0.01 degrees and 0.01 days. The technique used was to locate from the Nautical Almanac, the geographic longitude of the ascending node at epoch through the reported right ascension of the ascending node for the orbit, and the hour-angle of the vernal equinox calculated at epoch. The geographic longitude of the ascending equator crossing was then estimated by turning the earth back through the orbit angle from the ascending node to the satellite at epoch. This latter quantity was estimated as $\omega - M$ for the near-circular orbit of Syncom II. A correction factor to this orbit angle — the ratio of the satellite's period to the earth's sidereal period — was applied for orbits whose period was sufficiently different from the earth's. The nodal longitude at epoch, minus this reduced nodal excursion angle, is the estimated "ascending equator crossing nearest to epoch" reported in Table 1. (See Appendix E for an example of this calculation.)

Table 2 gives the Goddard-reported semimajor axes for these 27 orbits. Truncating equations (51) and (54A) at their first righthand terms:

$$\Delta\lambda \text{ (longitude drift from "synchronism")} \doteq -\left(A_{22} \sin 2\gamma_0\right)\frac{(\Delta t)^2}{2} \tag{63}$$

$$a_1 \text{ (semimajor axis change from "synchronism")} \doteq A_{22}\,\frac{\sin 2\gamma_0\,(\Delta t)}{3\pi} . \tag{64}$$

Let the drift time be given from a certain arbitrary base time by T. Let T_0 be the time of "synchronism" from the base time. Let the drift be given from a certain arbitrary geographic longitude by λ. Let λ_0 be the geographic longitude from this base longitude, of the "synchronous" configuration. Then:

$$\Delta t = T - T_0 , \text{ and}$$

$$\Delta\lambda = \lambda - \lambda_0 .$$

With these changes, (63) and (64) become $\left(\text{noting that } a_1 = \frac{a - a_s}{a_s}\right)$:

$$\lambda = \lambda_0 - \frac{(A_{22})\,(\sin 2\gamma_0)}{2}\left(T^2 - 2TT_0\,T_0^2\right) , \text{ or}$$

$$\lambda = \left\{\lambda_0 - \frac{T_0^2\left(A_{22} \sin 2\lambda_0\right)}{2}\right\} + T\left\{T_0\,A_{22} \sin 2\gamma_0\right\} + T^2\left\{-\frac{A_{22} \sin 2\gamma_0}{2}\right\}. \tag{65}$$

Table 1

Estimated Ascending Equator Crossings Nearest the Epoch of 27 Syncom II Orbits.

First Drift Orbit #	Time from 20.0 Aug. 1963 (days)	Ascending Equator Crossing in Degrees West of 50.0° West	Second Drift Orbit #	Time from 26.0 Nov. 1963 (days)	Ascending Equator Crossing in Degrees West of 50.0° West
1-1	2.12	4.89	2-1	1.86	9.17
1-2	7.11	4.83	2-2	7.84	9.17
1-3	11.09	4.78	2-3	13.83	9.22
1-4	16.08	4.74	2-4	20.81	9.38
1-5	20.07	4.77	2-5	41.75	10.15
1-6	23.06	4.78	2-6	44.74	10.36
1-7	28.05	4.85	2-7	55.71	11.02
1-8	31.04	4.90	2-8	64.69	11.76
1-9	38.02	5.06	2-9	71.67	12.32
1-10	42.01	5.09	2-10	76.66	12.81
1-11	48.99	5.45	2-11	83.64	13.49
1-12	54.97	5.68			
1-13	62.95	6.09			
1-14	70.93	6.60			
1-15	77.91	7.14			
1-16	83.90	7.61			
	~100.0	First free drift period ends at an ascending equator crossing of ~9.15° west of 50.0° west.			

Table 2

Goddard-Reported Semimajor Axes for 27 Syncom II Orbits.

First Drift Orbit #	Time from 20.0 Aug. 1963 (days)	Semimajor Axis: (42160.0 + Data; km)	Second Drift Orbit #	Time from 26.0 Nov. 1963 (days)	Semimajor Axis: (42160.0 + Data; km)
1-1	2.27	4.58	2-1	2.04	5.89
1-2	6.71	4.52	2-2	8.00	7.20
1-3	11.00	6.02	2-3	14.00	7.18
1-4	16.00	6.39	2-4	20.71	8.17
1-5	20.00	6.35	2-5	41.71	8.01
1-6	23.08	6.55	2-6	44.25	9.90
1-7	28.08	6.70	2-7	55.88	11.33
1-8	31.08	7.42	2-8	64.83	11.91
1-9	38.08	7.51	2-9	71.67	12.89
1-10	42.08	8.88	2-10	76.79	13.31
1-11	49.08	9.14	2-11	83.71	14.89
1-12	55.08	9.78			
1-13	63.08	11.51			
1-14	71.00	11.09			
1-15	78.00	12.15			
1-16	84.21	12.51			
	~100.0	First free drift period ends with a semimajor axis of ~42174.5 km.			

(Note that from (65), $\ddot{\lambda} = -A_{22} \sin 2\gamma_0 = \ddot{\gamma}_0$ from (33). This result is valid only for orbits sufficiently close to "synchronous," as discussed previously.)

$$a = a_s + a_s \left[\frac{A_{22} \sin 2\gamma_0}{3\pi}\right]\left[T - T_0\right] \quad , \text{ or}$$

$$a = a_s \left(1 - \frac{T_0 A_{22} \sin 2\gamma_0}{3\pi}\right) + T\left(\frac{a_s A_{22} \sin 2\gamma_0}{3\pi}\right) \quad . \tag{66}$$

(66) and (65) may be written with determinable coefficients as

$$\lambda = d_0 + d_1 T + d_2 T^2 \quad , \tag{67}$$

$$a = e_0 + e_1 T \quad , \tag{68}$$

where:

$$\begin{aligned} d_0 &= \lambda_0 - \frac{T^2 A_{22} \sin 2\gamma_0}{2} \quad , \\ d_1 &= \left(+ A_{22} T_0 \sin 2\gamma_0\right) \quad , \\ d_2 &= - \frac{A_{22} \sin 2\gamma_0}{2} \quad , \\ e_0 &= a_s \left(1 - \frac{T_0 A_{22} \sin 2\gamma_0}{3\pi}\right) \quad , \\ e_1 &= a_s A_{22} \frac{\sin 2\gamma_0}{3\pi} \end{aligned} \tag{69}$$

From (69),

$$T_0 = - d_1 / 2d_2 \quad , \tag{70}$$

$$\lambda_0 = d_0 - \frac{(d_1)^2}{4d_2} \quad , \tag{71}$$

$$\ddot{\gamma}_0 = - A_{22} \sin 2\gamma_0 = 2d_2 \quad . \tag{72}$$

Alternately, and as an internal check on the theory of the coupling of the drift and orbit expansion,

$$\ddot{\gamma}_0 = - A_{22} \sin 2\gamma_0 = \frac{-3\pi e_1}{a_s} \quad , \text{ implying}$$

$$d_2 = 3\pi e_1 / 2a_s \quad . \tag{73}$$

In equation (73), the units of d_2 must be radians/sidereal day^2, and the units of e_1 must be length/sidereal day so that the equation will be dimensionally correct. The semimajor axis at the "synchronous" configuration is calculated from (68) for $T = T_0$:

$$a_s = e_0 + e_1 T_0 \quad . \tag{74}$$

For the first drift period (orbits 1-1 through 1-16), the best estimates (in the "least squares" sense) of the coefficients $(d)_1$ and $(e)_1$, obtained by fitting (67) and (68) to the data in Tables 1 and 2, have been found to be:

$$(d_0)_1 = (4.941 \pm .018) \text{ degrees}$$

$$(d_1)_1 = -(.0216 \pm .0010) \text{ degrees/solar day}$$

$$(d_2)_1 = (6.37 \pm .11) \times 10^{-4} \text{ degrees/solar day}^2$$

$$= (6.33 \pm .11) \times 10^{-4} \text{ degrees/sid. day}^2$$

$$(e_0)_1 = (4.35 \pm .19) \text{ km}$$

$$(e_1)_1 = (.0993 \pm .0042) \text{ km/solar day}$$

$$(.0990 \pm .0042) \text{ km/sid. day} \quad .$$

The mean value of the inclination during this period was

$$(i)_1 = 33.018 \pm .005 \text{ degrees} \quad .$$

From (70),

$$(T_0)_1 = \left(16.95 \begin{smallmatrix} +1.09 \\ -1.05 \end{smallmatrix}\right) \text{ days from 20.0 August 1963} \quad .$$

From (71),

$$(\lambda_0)_1 = (4.76 \pm .03) \text{ degrees west of 50.0 degrees west longitude} \quad .$$

From (72),

$$(\ddot{\gamma}_0)_1 = -(1.27 \pm .02) \times 10^{-3} \text{ degrees/solar day}^2 = -(2.20 \pm .04) \times 10^{-6} \text{ rad./sid. day}^2 \quad .$$

From (74) and the above value of $(T_0)_1$,

$$(a_s)_1 = (42166.0 \pm .2) \text{ km} \quad .$$

For the second drift period (orbits 2-1 through 2-11), the best estimates (in the "least squares" sense) of the coefficients $(d)_2$ and $(e)_2$, obtained by fitting (67) and (68) to the data in Tables 1 and 2, have been found to be:

$$(d_0)_2 = (9.156 \pm .017) \text{ degrees}$$

$$(d_1)_2 = -(.0030 \pm .0010) \text{ degrees/solar day}$$

$$(d_2)_2 = (6.59 \pm .11) \times 10^{-4} \text{ degrees/solar day}^2$$

$$= (6.55 \pm .11) \times 10^{-4} \text{ degrees/sid. day}^2$$

$$(e_0)_2 = (5.70 \pm .42) \text{ km}$$

$$(e_1)_2 = (.0994 \pm .0080) \text{ km/solar day}$$

$$= (.0990 \pm .0080) \text{ km/sid. day .}$$

The mean value of the inclination during this period was

$$(i)_2 = 32.851 \pm .010 \text{ degrees .}$$

From (70),

$$(T_0)_2 = 2.3 \pm .8 \text{ days from 26.0 November 1963 .}$$

From (71),

$$(\lambda_0)_2 = 9.15 \pm .02 \text{ degrees west of 50.0 degrees west longitude .}$$

From (72),

$$(\ddot{\gamma}_0)_2 = -(1.32 \pm .02) \times 10^{-3} \text{ degrees/solar day}^2 = -(2.29 \pm .04) \times 10^{-6} \text{ rad./sid. day}^2 .$$

From (74) and the above value of $(T_0)_2$,

$$(a_s)_2 = (42165.9 \pm .4) \text{ km .}$$

(See Figure 5 for a graph of this orbit data and reduction for the two drift periods.) Combining the above results of the two free-drift periods, from (61),

$$\frac{(A_{22})_1}{(A_{22})_2} = (42165.9 \pm .4/42166.0 \pm .2)^2 \frac{[\cos^2 (33.018 \pm .005) + 1]}{[\cos^2 (32.851 \pm .010) + 1]}$$

$$= .99845 \pm .00014 .$$

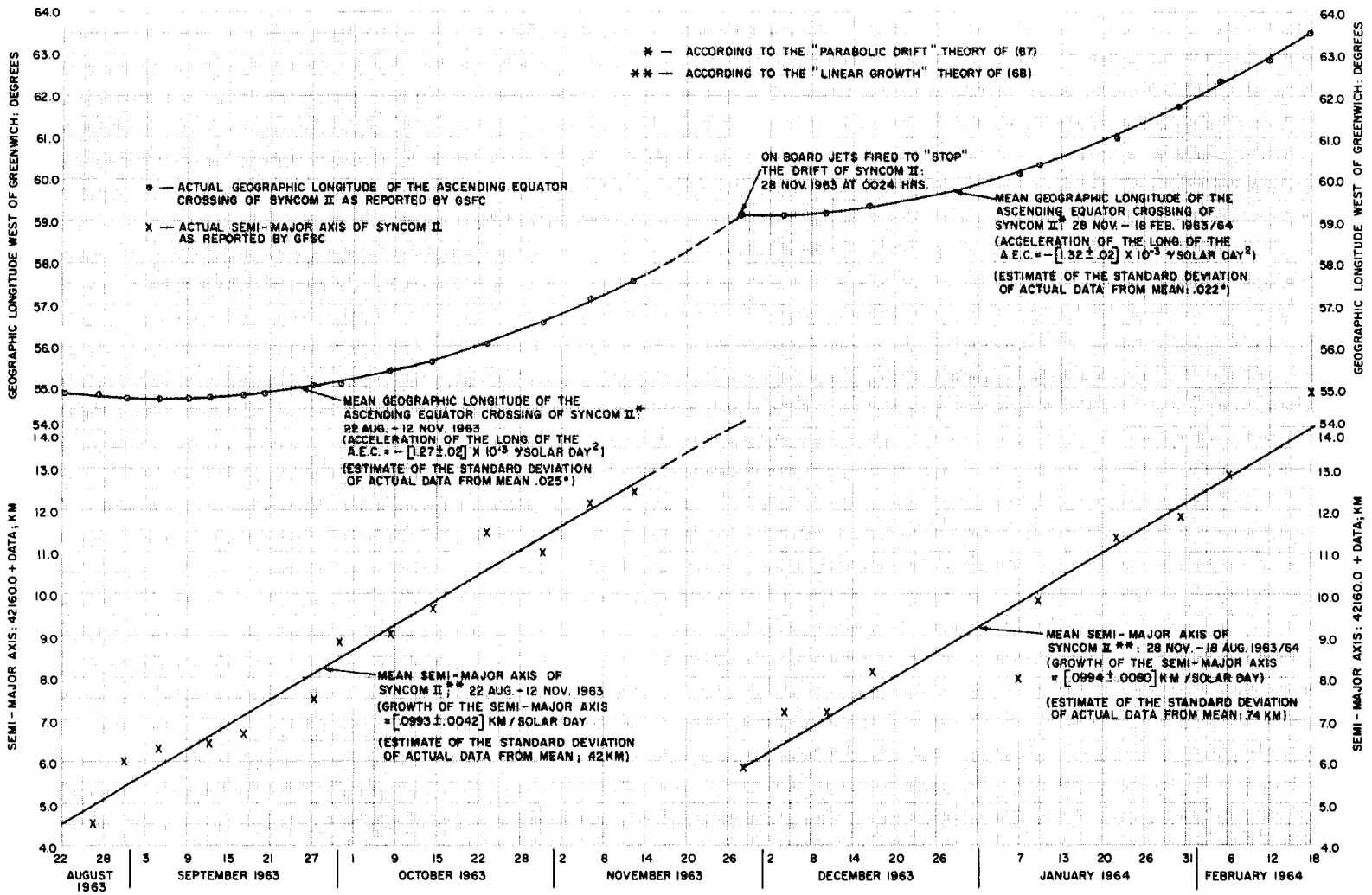

Figure 5—Drift of the ascending equator crossing and growth of the semimajor axis of Syncom II.

The longitude separation between the two drift periods is given by

$$\nabla\lambda = (\lambda_0)_2 - (\lambda_0)_1 = \left[-(59.15 \pm .02)\right] - \left[-(54.76 \pm .03)\right] \text{ degrees}$$

$$= -(4.39 \pm .05) \text{ degrees geographic longitude .}$$

Thus

$$2\nabla\lambda = -(8.78 \pm .10) \text{ degrees geographic longitude .}$$

Therefore, from (59), the location of the minor equatorial axis with respect to the "synchronous" longitude during the first free-drift period (54.76 ± .03 degrees west of Greenwich) is

$$(\gamma_0)_1 = \frac{1}{2}\tan^{-1}\left\{\frac{\sin\left[-(8.78 \pm .10)\right]}{\frac{(1.32 \pm .02)}{(1.27 \pm .02)}(.99845 \pm .00014) - \cos\left[-(8.78 \pm .10)\right]}\right\}$$

$$= 54\,{}^{+4}_{-6} \text{ degrees east of the minor equatorial axis .}$$

From (61B), the best estimate of the location of the major equatorial axis is

$$\lambda_{22} = -55 - \left(54\,{}^{+4}_{-6}\right) + 90 = -\left(19\,{}^{+4}_{-6}\right) \text{ degrees geographic longitude .}$$

From (60), the best estimate of the triaxial gravity coefficient J_{22} is

$$J_{22} = \frac{-(2.20 \pm .04) \times 10^{-6}}{72\pi^2\left[\sin 2\left(54\,{}^{+4^\circ}_{-6^\circ}\right)\right](6378.2/42166.0 \pm .3)^2\left[\frac{\cos^2(33.018 \pm .005) + 1}{2}\right]}$$

$$= -\left(1.67\,{}^{+.07}_{-.03}\right) \times 10^{-6} .$$

The mean equatorial radius, taken as $R_0 = 6378.2$ km, is a compromise between a number of currently used values. It is stated above without error. The likely error in $(a_s)_1$ has been increased arbitrarily by 0.1 km. to account for the likely uncertainty in R_0.

Using the above estimate of J_{22} from observations on Syncom II drift, the difference between the major and minor equatorial radii of the triaxial geoid is, by (62),

$$a_0 - b_0 = 64\,{}^{+3}_{-1} \text{ meters} = 210\,{}^{+10}_{-4} \text{ feet .}$$

Comparing the deviation due to earth ellipticity with other higher order earth-gravity deviations (Appendix B and Reference 10), we note that the above figure implies a maximum deviation

from the mean earth sphere, due to the ellipticity of the equator, of

$$\Delta R_0 = 105 \, {}^{+5}_{-2} \text{ feet} .$$

REFERENCES

1. Heiskanen and Meinesz: 1958, *The Earth and Its Gravity Field,* (Mcgraw-Hill)

2. Izsak: July, 1963, "Tesseral Harmonics In The Geopotential," *Nature* July 13, 1963, pp. 137-139

3. Blitzer, Boughton, Kang and Page: 1962, "Effect of Ellipticity of the Equator On 24-Hour Nearly Circular Satellite Orbits," *Journal of Geophysical Research,* Vol. 67, pp. 329-335

4. Frick and Garber: 1962, private communication (Rand Corp. Memo. RM-2296)

5. Barrett: 1962, "The Perturbations of a Synchronous Satellite Resulting From The Gravitational Field of a Triaxial Earth," GSFC Document X-623-62-160, Sept. 10, 1962, NASA

6. Wagner: 1964, "The Drift of a 24-Hour Equatorial Satellite Due To An Earth Gravity Field Through 4th Order," NASA TN-D-2103, Feb. 1964

7. Musen: 1962, "On The Motion Of A 24-Hour Satellite," *Journal of Geophysical Research,* Vol. 67 #3, pp. 1123-1132

8. Thomson: 1961, *Introduction To Space Dynamics,* p. 72 (John Wiley and Sons)

9. Isley: 1962, "A Summary of Constants Associated With Orbital Analysis of Earth Satellites, Including the Influence Of Their Uncertainties Upon Gravitational Measurements For Synchronous Satellites," GSFC Document X-623-62-169

10. Wagner: 1962, "The Gravitational Potential of a Triaxial Earth," GSFC Document X-623-62-206, Oct. 62, NASA

11. Salvadori and Schwarz: 1954, *Differential Equations In Engineering Problems,* Chapter 9 (Prentice Hall)

12. Jahnke and Emde: 1945 ed., *Tables Of Functions,* Chapter V (Dover Publications)

13. Kozai: 1961, "The Earth's Gravitational Potential Derived from Motions of Three Satellites," *Astronomical Journal,* Vol. 66, pp. 8-10

14. O'Keefe, Eckels and Squires: 1959, "The Gravitational Field of the Earth," *Astronomical Journal,* vol. 64, pp. 245-253

LIST OF SYMBOLS

J_{nm}, λ_{nm} Spherical harmonic constants (order n, power m) of the earth's gravity potential

F A gravity force per unit mass acting on a 24-hour satellite

θ (except in Appendix F) The argument from the ascending node to the satellite position for the 24-hour orbit

a, a_s The instantaneous semimajor axis, and the "momentarily synchronous" semimajor axis of the orbit of the 24-hour earth satellite. (a_s, estimated to within 2 km, is 42166 km.)

ds A small arc length of a space trajectory

μ_E The earth's gaussian gravity constant (3.986×10^5 $km^3/sec.^2$)

T_p, T_s The orbital period for a satellite, and the "momentarily synchronous" period of a 24-hour satellite (i.e., the earth's sidereal rotation period)

λ, r, ϕ Geographic longitude, geocentric radius, and geocentric latitude of the 24-hour satellites position

$(\dot{}), (\ddot{}), ( )^n$ $\frac{d( )}{dt}$, $\frac{d^2( )}{dt^2}$, $\frac{d^n( )}{dt^n}$: time differentials

R_0 The mean equatorial radius of the earth (6378.2 km)

i The inclination of the orbit of the 24-hour satellite

λ_0 The "initial" geographic longitude of the satellite, or the ascending node of the 24-hour satellite's orbit at the start of the dynamics under consideration

w_e The earth's sidereal rotation rate ($.7292115 \times 10^{-4}$ rad./sec.)

t Real time

$\Delta( )$ A small argument ( )

γ_0 The geographic longitude (positive to the east) of the ascending node of the 24-hour satellite's orbit with respect to the earth's minor equatorial axis' longitude location, at the start of the dynamics under consideration

γ The geographic longitude (positive to the east) of the 24-hour satellite, or the ascending node of the satellite's orbit with respect to the longitude of the earth's minor equatorial axis

a_1 $(a - a_s)/a_s$; a nondimensional semimajor axis change for the 24-hour satellite's orbit, with respect to the "momentarily synchronous" semimajor axis

A_{22} The driving function causing drift and orbit expansion of a 24-hour satellite in a "triaxial" earth-gravity field; a constant for a given 24-hour orbit inclination

$( )_0$ The argument ( ) at the start of the dynamics under consideration

$( )_n$ The argument ( ) at a specified location n (except in Appendix A: ( )s; the argument for the simulated trajectory)

$\nabla\lambda$ The geographic longitude difference between two "momentarily synchronous" 24-hour satellite configurations

a_0, b_0 The major and minor equatorial radii of the "triaxial" earth $\left(R_0 = \frac{a_0 + b_0}{2}\right.$, according to the definition in Reference 10$\left.\right)$

w The argument of perigee in a satellite orbit: The orbit angle (from the center of the earth) from the ascending node to perigee

M The mean anomaly of the satellite in its orbit: The orbit angle (from the center of the earth) from perigee to a point M in the orbit, where $M = \frac{2\pi t}{T_p}$, t being the real time since perigee passage and T_p the period of the satellite's orbit

$(e_n), (d_n)$ Determinable coefficients in the drift and orbit-expansion equations (67) and (68)

T_0 The time of "synchronism" from an arbitrary base time of reckoning T

F(i) The inclination factor in the triaxial driving function A_{22}

V_E The gravity potential of the earth

g_0, g_s The radial acceleration of the earth's gravity field at the earth's surface, and at the altitude of the "synchronous" satellite

m A test mass

$F(\underline{k}, \phi)$ The elliptic integral of the first kind with argument (or amplitude) ϕ and modulus $\underline{k}$

Λ The longitude location of the vernal equinox

Appendix A

REDUCTION OF SIMULATED PARTICLE TRAJECTORIES FOR EARTH EQUATORIAL ELLIPTICITY

Tables A-1 and A-2 present data taken from a numerically integrated particle trajectory of a triaxial earth in the presence of the sun and moon's gravity field. Only perturbed equations of motion from a periodically rectified Keplerian reference orbit are actually integrated by the digital computer program (called ITEM at the Goddard Space Flight Center). For the 3 months' real orbit time of these trajectories, the accumulated truncation and roundoff error in the numerical integration is believed to be negligible for the purposes of this reduction. The initial position and velocity conditions for these simulated trajectories were the same as those reported for the "actual" Syncom II orbits 1-2 (for the trajectory of Table A-1) and 2-3 (for the trajectory of Table A-2). The program used the earth gaussian-gravity constant

$$\mu_E = 3.9862677 \times 10^5 \text{ km}^3/\text{sec}^2 ,$$

which is the gravity constant used by the GSFC Data and Tracking Systems Directorate in computing the elements of satellite orbits from radar and Minitrack observations. The best estimates (in the "least squares" sense) of the coefficients $(d)_{s1}$ and $(e)_{s1}$, obtained by fitting the drift and orbit expansion equations (67) and (68) to the data in Table A-1, have been found to be

$$(d_0)_{s1} = 4.841 \pm .004 \text{ degrees}$$

$$(d_1)_{s1} = -(1.22 \pm .03) \times 10^{-2} \text{ degrees/solar day}$$

$$(d_2)_{s1} = (6.303 \pm .038) \times 10^{-4} \text{ degrees/solar day}^2$$

$$= (6.268 \pm .038) \times 10^{-4} \text{ degrees/sid. day}^2$$

$$(e_0)_{s1} = 5.45 \pm 41 \text{ km}$$

$$(e_1)_{s1} = (.091 \pm .010) \text{ km/solar day}$$

$$= (.091 \pm .010) \text{ km/sid. day} .$$

The mean value of the inclination during this first simulated trajectory period was

$$(i)_{s1} = 33.005 \pm .003 \text{ degrees} .$$

Table A-1

Data from Simulated Trajectory Beginning with the Elements of Syncom II Orbit 1-2.

($J_{22} = -1.68 \times 10^{-6}, R_0 = 6378.388$ km, $\gamma_{22} = -108.0$: Input into Trajectory Program)

Time from 26.709 Aug. 1963: (Solar Days)	Ascending Equator Crossing: (Degrees West of 50.0° West Geog. Long.)	Semimajor Axis (42160.0 + Data; km)	Inclination (32.0 + Data; Degrees)
2.390	4.816	5.27	1.089
8.374	4.783	7.09	1.072
14.358	4.792	6.01	1.056
20.341	4.861	8.12	1.043
26.324	4.954	7.13	1.025
32.308	5.101	8.98	1.019
38.292	5.291	8.31	.997
44.276	5.537	9.67	.991
47.268	5.678	10.38	.983
50.260	5.821	10.03	.972
53.253	5.975	9.42	.967
56.245	6.144	9.74	.966
59.237	6.326	11.09	.960
62.229	6.522	11.94	.957

Table A-2

Data from Simulated Trajectory Beginning with the Elements of Syncom II Orbit 2-3.

($J_{22} = -1.68 \times 10^{-6}$, $R_0 = 6378.388$ km, $\gamma_{22} = -108.0$: Input into Trajectory Program)

Time from 10.0 Dec. 1963: (days)	Ascending Equator Crossing: (Degrees West of 50.0° West Geog. Long.)	Semimajor Axis (42160.0 + Data; km)	Inclination (32.0 + Data; Degrees)
0.823	9.243	6.88	.881
5.809	9.351	7.30	.881
10.796	9.495	9.41	.877
15.783	9.666	8.15	.864
20.769	9.885	9.85	.864
25.756	10.134	10.60	.850
30.743	10.401	9.95	.842
35.730	10.708	11.81	.841
40.717	11.044	12.18	.825
45.704	11.412	11.58	.816
50.692	11.830	13.93	.808
55.679	12.259	13.11	.790
58.672	12.534	13.07	.785
60.667	12.724	13.69	.784

From (70),

$$(T_0)_{s1} = 9.68 \pm .30 \text{ days from 26.709 August 1963}$$

From (71),

$$(\triangle_0)_{s1} = 4.782 \begin{matrix} +.008 \\ -.007 \end{matrix} \text{ degrees west of 50.0 degrees west longitude .}$$

From (72),

$$(\ddot{\gamma}_0)_{s1} = -(1.261 \pm .008) \times 10^{-3} \text{ degrees/solar day}^2$$

$$= -(2.188 \pm .013) \times 10^{-6} \text{ rad./sid. day}^2 .$$

From (74) and the above value of $(T_0)_{s1}$,

$$(a_s)_{s1} = 42166.3 \pm .4 \text{ km} .$$

The best estimates (in the "least squares" sense) of the coefficients $(d)_{s2}$ and $(e)_{s2}$, obtained by fitting the drift and orbit expansion equations (67) and (68) to the data in Table A-2, have been found to be

$$(d_0)_{s2} = 9.224 \pm .004 \text{ degrees}$$

$$(d_1)_{s2} = (1.830 \pm .028) \times 10^{-2} \text{ degrees/solar day}$$

$$(d_2)_{s2} = (6.501 \pm .042) \times 10^{-4} \text{ degrees/solar day}^2$$

$$= (6.465 \pm .042) \times 10^{-4} \text{ degrees/sid. day}^2$$

$$(e_0)_{s2} = 7.19 \pm .37 \text{ km}$$

$$(e_1)_{s2} = (.111 \pm .010) \text{ km/solar day}$$

$$= (.111 \pm .010) \text{ km/sid. day} .$$

The mean value of the inclination during the second simulated trajectory period is

$$(i)_{s2} = 32.836 \pm .003 \text{ degrees} .$$

From (70),

$$(T_0)_{s2} = -(14.07 \pm .30) \text{ days from 10.0 December 1963} .$$

From (71),

$$(\triangle_0)_{s2} = 9.095 \begin{matrix} +.009 \\ -.009 \end{matrix} \text{ degrees west of 50.0 degrees west longitude .}$$

From (72),

$$(\ddot{\gamma}_0)_{s2} = -(1.300 \pm .008) \times 10^{-3} \text{ degrees/solar day}^2$$

$$= -(2.257 \pm .015) \times 10^{-6} \text{ rad./sid. day}^2 .$$

From (74) and the above value of $(T_0)_{s2}$,

$$(a_s)_{s2} = 42165.6 \pm .5 \text{ km} .$$

A graph of these trajectory simulations is seen in Figure A-1.

Combining the above results for the two simulated trajectories: from (61),

$$\frac{(A_{22})_{s1}}{(A_{22})_{s2}} = \left[(42165.6 \pm .5/42166.3 \pm .4)^2\right] \left[\frac{\cos^2 (33.005 \pm .003) + 1}{\cos^2 (32.836 \pm .003) + 1}\right]$$

$$= .99840 \bullet .00007$$

$$\nabla\lambda = (\lambda_0)_{s2} - (\lambda_0)_{s1} = \left[-(59.095 \pm .009)\right] - \left[-(54.782 \pm .008)\right] ,$$

$$\therefore 2\nabla\lambda = -(8.626 \pm .034) \text{ degrees geographic longitude} .$$

Therefore, from (59), the location of the minor equatorial axis with respect to the "synchronous longitude" during the first simulated trajectory (54.782 ± .008 degrees west of Greenwich) is

$$(\gamma_0)_{s1} = \frac{1}{2} \tan^{-1} \left\{ \frac{\sin \left[-(8.626 \pm .034)\right]}{\frac{(1.300 \pm .008)}{(1.261 \pm .008)} (.99840 \pm .00007) - \cos \left[-(8.626 \pm .034)\right]} \right\}$$

$$= 52.5 \pm 2.5 \text{ degrees east of the minor equatorial axis} .$$

From (61A), the best estimate of the geographic location of the nearest extension of the equatorial minor axis from the simulated trajectory data is

$$(\gamma_{22})_s = -54.8 - (52.5 \pm 2.5) = -(107.3 \pm 2.5) \text{ degrees geographic longitude} .$$

This compares well with the input value of $(\gamma_{22})_s = -108.0°$ used to compute the simulated trajectories. From (60), the best estimate of the triaxial gravity coefficient J_{22} from the simulated data (according to the theory of this report) is

$$(J_{22})_s = \left\{ \frac{-(2.188 \bullet .013) \times 10^{-6}}{72\pi^2 \left[\sin 2(52.5 \pm 2.5)\right] (6378.388/42166.3 \pm .4)^2 \left[\frac{\cos^2 (33.005 \pm .003) + 1}{2}\right]} \right\}$$

$$= -(1.64 \bullet .03) \times 10^{-6} .$$

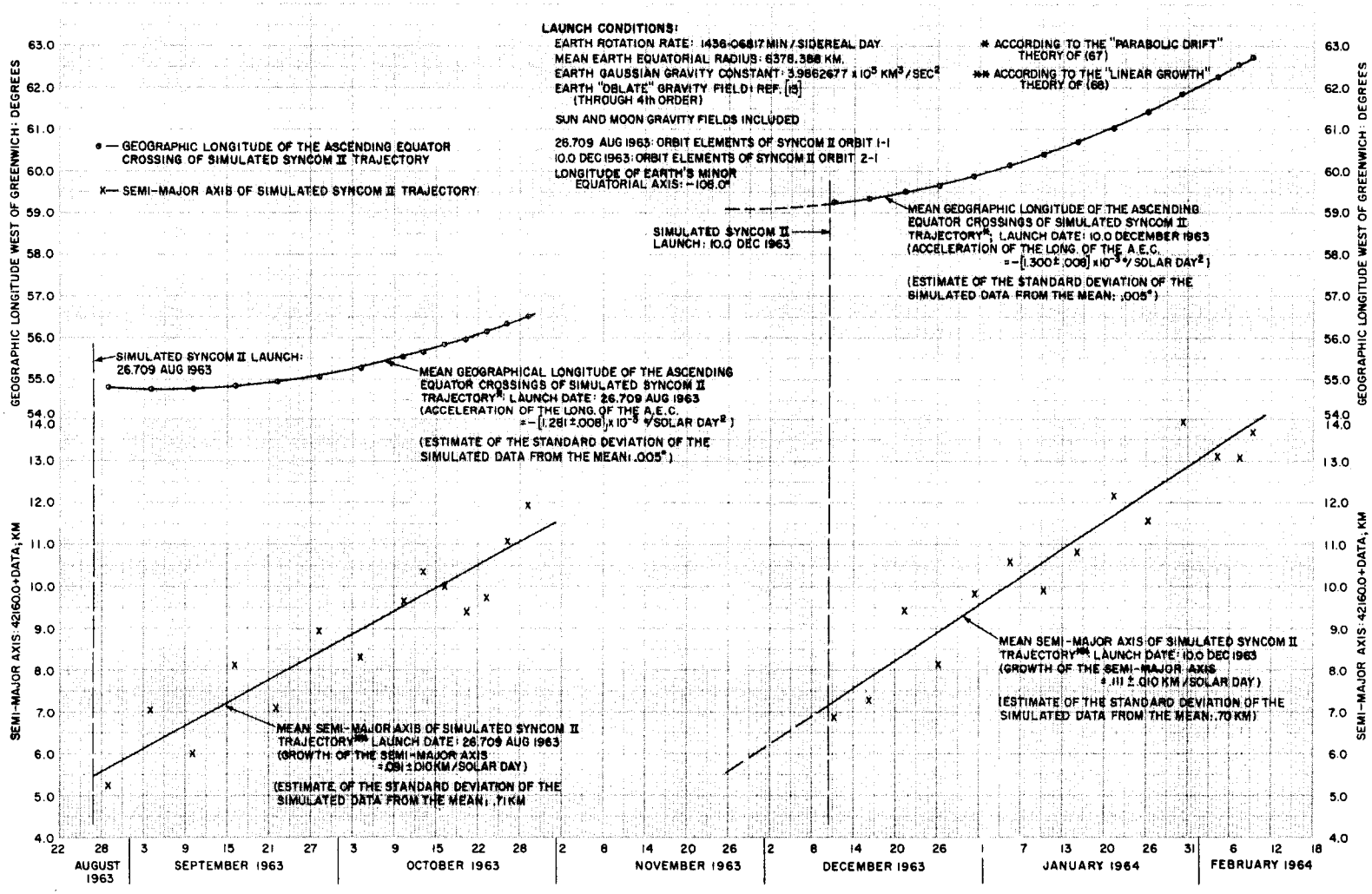

Figure A-1—Drift of the ascending equator crossing and growth of the semimajor axis of simulated Syncom II trajectories.

The mean equatorial radius used in the simulation is R_0 = 6378.388 km, the same used to compute the "actual" Syncom II orbits from the radar and Minitrack observations.

The above value of $(J_{22})_s$ compares reasonably well with the input value of $(J_{22})_s = -(1.68) \times 10^{-6}$ used to compute the simulated trajectories.

The model error implicit in the difference between the reduced and inputed geodetic coefficients for the simulated trajectories warrants an adjustment of the J_{22} and λ_{22} reported in Section 7 from the reduction of the "actual" Syncom II orbits. The values below appear sufficient to cover all the *known* uncertainties of this reduction for a triaxial earth:

$$J_{22} \text{ (actual-adjusted)} = -(1.70 \pm .05) \times 10^{-6}$$

$$\lambda_{22} \text{ (actual-adjusted)} = -(19 \pm 6) \text{ degrees geographic longitude .}$$

As Appendix B will show, the principal *unknown* uncertainty of the reduction is the possible influence of higher order earth tesseral anomalies on the drift of Syncom II. When all relevant higher order anomalies in the earth's gravity potential are evaluated, the adjusted values above will probably remain representative for an "average" triaxial potential field sufficient to consider for the future design of synchronous satellites. As a guess, the author would increase the upper limit of J_{22} to about $-(1.80) \times 10^{-6}$ (based on some of the recent gravity potentials in Appendix B) for design purposes, based on an "average" triaxial geoid. A lower limit of $J_{22} = 1.60 \times 10^{-6}$ for this purpose appears justifiable. The variance in the location of the major equatorial axis for the "average" triaxial geoid is not likely to change appreciably from the value quoted for the adjusted figure. The author is presently studying these higher order earth-gravity effects. The accumulated influence on synchronous satellites of all higher order earth anomalies, is believed to be small compared to the 2nd order anomaly. But it appears that close and continuing observations on the drift of these satellites will be rewarded in time by revelation of many of these "tesseral" anomalies to about 4th order with an absolute precision almost as good as that reported here for the 2nd order effect.

Appendix B

THE EARTH GRAVITY POTENTIAL AND FORCE FIELD USED IN THIS REPORT: COMPARISON WITH PREVIOUS INVESTIGATIONS

The gravity potential used as the basis for the data reduction in this study is the exterior potential of the earth derived in reference 10 for geocentric spherical coordinates referenced to the earth's spin axis and its center of mass. The infinite series of spherical harmonics is truncated after J_{44}. The nontesseral harmonic constants J_{20}, J_{30} and J_{40} are derived from reference 13.

The earth radius R_0 used in this study is:

$$R_0 = 6378.388 \text{ km} .$$

The earth's gaussian gravity constant used is:

$$\mu_E = 3.9862677 \times 10^5 \text{ km}^3/\text{sec}^2 .$$

Neither of these values, taken from reference 14, nor the "zonal geoid" of Reference 13, is felt to be the most accurate known to date. They are the values used by the GSFC Tracking and Data Systems Directorate to calculate the orbit elements of Syncom II from radar and Minitrack observations. They were chosen to insure consistency between the data of this study and these published orbits, inasmuch as the "triaxial" reduction for which this study has been undertaken is not significantly affected by the probable errors in these values. The second-order tesseral harmonic constants used in the simulation studies were

$$J_{22} = -1.68 \times 10^{-6}$$

$$\lambda_{22} = -18^\circ .$$

These are the values shown on the "tesseral geoid" below (for the J_{22} harmonic). At a later point in the analysis, the slightly different values reported in the abstract were estimated. The most accurate "zonal geoid" is probably that of Kozai (1962) [See Reference 6], with the following earth constants;

$$R_0 = 6.378.2 \text{ km}$$

$$\mu_E = 3.98603 \times 10^5 \text{ km}^3/\text{sec}^2 .$$

The earth's gravity potential (to fourth order, probably sufficient to account for all significant perturbations on a 24-hour satellite) may be illustrated as follows (following Reference 6, Appendix B):

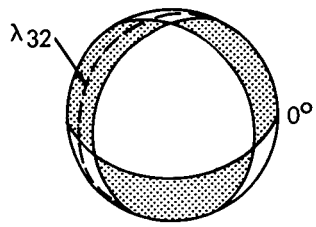

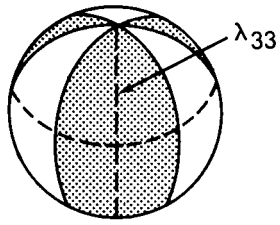

$$-15J_{32}\frac{R_o^3}{r^3}\cos^2\phi\sin\phi\cos\,2(\lambda-\lambda_{32}) - 15J_{33}\frac{R_o^3}{r^3}\cos^3\phi\cos\,3(\lambda-\lambda_{33})$$

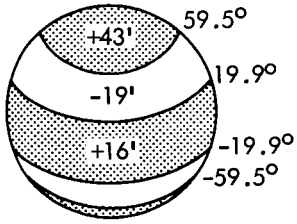

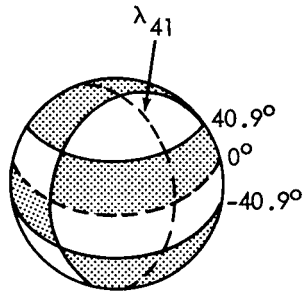

$$-\frac{J_{40}R_o^4}{8r^4}\left(35\sin^4\phi - 30\sin^2\phi + 3\right) - \frac{J_{41}R_o^4}{8r^4}\left[140\sin^3\phi - 60\sin\phi\right]\cos\phi\cos\left(\lambda-\lambda_{41}\right) \qquad \text{(B-1)}$$

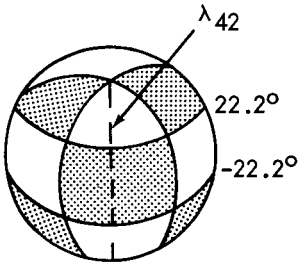

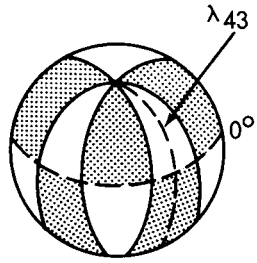

$$-\frac{J_{42}R_o^4}{8r^4}\left[420\sin^2\phi - 60\right]\cos^2\phi\cos\,2(\lambda-\lambda_{42}) - \frac{J_{43}R_o^4}{8r^4}\,840\sin\phi\cos^3\phi\cos\,3(\lambda-\lambda_{43})$$

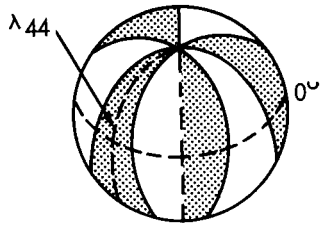

$$-\frac{J_{44}R_o^4}{8r^4}\,840\cos^4\phi\cos 4(\lambda-\lambda_{44})\Bigg\}$$

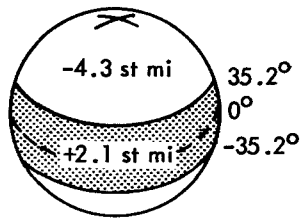

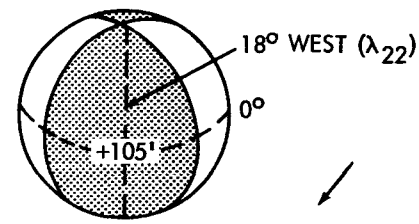

$$V_E = \frac{\mu_E}{r}\left\{1 - \frac{J_{20}R_o^2}{2r^2}\left(3\sin^2\phi - 1\right) - 3J_{22}\frac{R_o^2}{r^2}\cos^2\phi\cos 2\left(\lambda - \lambda_{22}\right)\right.$$

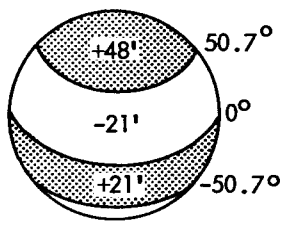

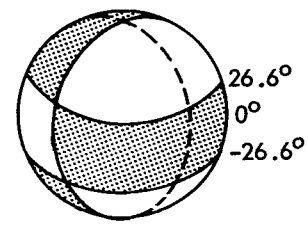

$$\left. - \frac{J_{30}R_o^3}{2r^3}\left(5\sin^3\phi - 3\sin\phi\right) - \frac{J_{31}R_o^3}{2r^3}\cos\phi\cos\left(\lambda - \lambda_{31}\right)\left(15\sin^2\phi - 3\right)\right.$$

The earth-gravity field (per unit test mass) whose potential is (B-1) is given as the gradient of (B-1), or

$$\bar{F} = \hat{r}F_r + \hat{\lambda}F_\lambda + \hat{\phi}F_\phi = \nabla V_E = \hat{r}\frac{\partial V_E}{\partial r} + \frac{\hat{\lambda}}{r\cos\phi}\frac{\partial V_E}{\partial\lambda} + \frac{\hat{\phi}}{r}\frac{\partial V_E}{\partial\phi}, \qquad \text{(B-2)}$$

or

$$\begin{aligned} F_r = \frac{\mu_E}{r^2}\Big\{ & -1 + \left(R_0/r\right)^2\left[3/2J_{20}\left(3\sin^2\phi - 1\right) + 9J_{22}\cos^2\phi\cos 2\left(\lambda - \lambda_{22}\right)\right. \\ & + 2\left(R_0/r\right)J_{30}\left(5\sin^2\phi - 3\right)\left(\sin\phi\right) + 6\left(R_0/r\right)J_{31}\left(5\sin^2\phi - 1\right)\cos\phi\cos\left(\lambda - \lambda_{31}\right) \\ & + 60\left(R_0/r\right)J_{32}\cos^2\phi\sin\phi\cos 2\left(\lambda - \lambda_{32}\right) + 60\left(R_0/r\right)J_{33}\cos^3\phi\cos 3\left(\lambda - \lambda_{33}\right) \\ & + 5/8\left(R_0/r\right)^2 J_{40}\left(35\sin^4\phi - 30\sin^2\phi + 3\right) \\ & + 25/2\left(R_0/r\right)^2 J_{41}\left(7\sin^2\phi - 3\right)\cos\phi\sin\phi\cos\left(\lambda - \lambda_{41}\right) \\ & + 75/2\left(R_0/r\right)^2 J_{42}\left(7\sin^2 - 1\right)\cos^2\phi\cos 2\left(\lambda - \lambda_{42}\right) \\ & \left. + 525\left(R_0/r\right)^2 J_{43}\cos^3\phi\sin\phi\cos 3\left(\lambda - \lambda_{43}\right) + 525\left(R_0/r\right)^2 J_{44}\cos^4\phi\cos 4\left(\lambda - \lambda_{44}\right)\right]\Big\} . \end{aligned} \qquad \text{(B-3)}$$

$$F_\lambda = \frac{\mu_E}{r^2}(R_0/r)^2 \left\{6J_{22}\cos\phi \sin 2(\lambda-\lambda_{22}) + 3/2\,(R_0/r)\,J_{31}\left[5\sin^2\phi - 1\right]\sin(\lambda-\lambda_{31})\right.$$

$$+ 30\,(R_0/r)\,J_{32}\cos\phi\sin\phi\sin 2(\lambda-\lambda_{32}) + 45\,(R_0/r)\,J_{33}\cos^2\phi\sin 3(\lambda-\lambda_{33})$$

$$+ 5/2\,(R_0/r)^2 J_{41}\left[7\sin^2\phi - 3\right]\sin\phi\sin(\lambda-\lambda_{41}) + 15\,(R_0/r)^2 J_{42}\left(7\sin^2\phi - 1\right)\cos\phi\sin 2(\lambda-\lambda_{42}) \quad \text{(B-4)}$$

$$+ 315\,(R_0/r)^2 J_{43}\cos^2\phi\sin\phi\sin 3(\lambda-\lambda_{43})$$

$$\left. + 420\,(R_0/r)^2 J_{44}\cos^3\phi\sin 4(\lambda-\lambda_{44})\right\}.$$

$$F_\phi = \frac{\mu_E}{r^2}(R_0/r)^2 \left\{-3J_{20}\sin\phi\cos\phi + 6J_{22}\cos\phi\sin\phi\cos 2(\lambda-\lambda_{22})\right.$$

$$- 3/2\,(R_0/r)\,J_{30}\left(5\sin^2\phi - 1\right)\cos\phi + 3/2\,(R_0/r)\,J_{31}\left(15\sin^2\phi - 11\right)\sin\phi\cos(\lambda-\lambda_{31})$$

$$+ 15\,(R_0/r)\,J_{32}\left(3\sin^2\phi - 1\right)\cos\phi\cos 2(\lambda-\lambda_{32})$$

$$+ 45\,(R_0/r)\,J_{33}\cos^2\phi\sin\phi\cos 3(\lambda-\lambda_{33}) - 5/2\,(R_0/r)^2 J_{40}\left(7\sin^2\phi - 3\right)\sin\phi\cos\phi \quad \text{(B-5)}$$

$$+ 5/2\,(R_0/r)^2 J_{41}\left(28\sin^4\phi - 27\sin^2\phi + 3\right)\cos(\lambda-\lambda_{41})$$

$$+ 30\,(R_0/r)^2 J_{42}\left(7\sin^2\phi - 4\right)\cos\phi\sin\phi\cos 2(\lambda-\lambda_{42})$$

$$+ 105\,(R_0/r)^2 J_{43}\left(4\sin^2\phi - 1\right)\cos^2\phi\cos 3(\lambda-\lambda_{43})$$

$$\left. + 420\,(R_0/r)^2 J_{44}\cos^3\phi\sin\phi\cos 4(\lambda-\lambda_{44})\right\}.$$

The actual sea-level surface of the earth is to be conceptualized through (B-1) as a sphere of radius 6378 km, around which are superimposed the sum of the separate spherical harmonic deviations illustrated. To these static gravity deviations, of course, must be added a centrifugal earth-rotation potential at the earth's surface, to get the true sea level surface (see Reference 10).

From Table B-1 and equation (B-3), the fourth-order tesseral geoids of Kaula (September 1963), Kozai (1962), Izsak (July 1963), and Zhongolovitch (1957) have been evaluated for the longitudinal perturbation force on a 24-hour satellite with zero inclination at $\lambda = -54.75°$ over the earth's surface (see Table B-2). The harmonics contributing to this perturbation are J_{22}, J_{31}, J_{33}, J_{42} and J_{44}. The results of this comparison are:

Table B-1

Tesseral Coefficients in the Earth's Gravity Potential, To Fourth Order, As Reported 1915-1963.*

	J_{22}	λ_{22}	J_{31}	λ_{31}	J_{32}	λ_{32}	J_{33}	λ_{33}	J_{41}	λ_{41}	J_{42}	λ_{42}	J_{43}	λ_{43}	J_{44}	λ_{44}
(1) Guier (Nov. 1963)	-1.80×10^{-6}	-10.4°	-1.77×10^{-6}	6.3°	$-.286 \times 10^{-6}$	-2.6°	$-.204 \times 10^{-6}$	24.1°	$-.73 \times 10^{-6}$	219°	$-.273 \times 10^{-6}$	38.6°	$-.0791 \times 10^{-6}$	-.7°	$-.0102 \times 10^{-6}$	35.0°
(2) Kaula (Sept. 1963)	-1.51	-18.1	-1.65	+5.3	-.144	46.4	-.145	15.8	-.471	132	-.078	44.2	-.0265	22.6	-.0038	23.3
(3) Izsak (July 1963)	-1.05	-11.2	-1.1	+3.2	-.20	-21.8	-.14	20.0	-.43	-132.1	-.13	37.0	-.026	11.5	-.019	14.8
(4) Kaula (May 1963)	-1.4	-21.5	-1.6	-1.9	-.15	35.8	-.12	18.5	-.53	+126.3	-.12	44.5	-.019	10.7	-.0038	23.3
(5) Cohen (May 1963)	-2.08	-14.1							-.775	201	-.288	34.6	-.162	-4.3		
(6) Kaula (Jan. 1963)	-1.62	-21.4	-1.81	-3.57	-.145	6.6	-.112	37.6	-.479	114.5	-.072	47.7	-.0988	5.9	-.0132	28.4
(7) Kozai (Oct. 1962)	-1.2	-26.4	-1.9	+4.6	-.14	-16.8	-.10	42.6	-.52	-122.5	-.062	65.2	-.035	0.5	-.031	14.9
(8) Newton (April 1962)	-2.15	-10.9							-2.53	+170.9						
(9) Newton (Jan. 1962)	-4.16	-11.0														
(10) Kozai (June 1961)	-2.32	-37.5	-3.95	+22.0	-.41	+31.0	-1.91	51.3	-.264	+163.5	-.167	54.0	-.046	-13.0	-.056	50.3
(11) Kaula (June 1961)	-.55	-13.3	-2.39	20.6	-.66	-.9	-.46	22.6	-1.85	194	-.42	21.1	-.091	-.5	-.024	26.4
(12) Izsak (Jan. 1961)	-5.35	-33.15														
(13) Kaula (1961)	-1.68	-38.5							-1.15	-13.0						
(14) Krassowski (1961?)	-5.53	+15.0														
†(15) Kaula (1959)	-.62	-20.9	-.98	55.4	-.11	13.3	-.19	14.3	-.46	-132.3	-.081	48.6	-.01	-30.0	-.02	22.5
†(16) Jeffreys (1959)	-4.17	0														
†(17) Uotila (1957)	-3.5	-6.0														
†(18) Zhongolovitch (1957)	-5.95	-7.7	-2.21	-25.7	-.628	-26.4	-.54	13.0	-.78	-149.1	-.080	45.0	-.051	-3.8	-.0224	15.9
†(19) Subbotin (1949)	-5.5															
†(20) Niskanen (1945)	-7.67	-4.0														
†(21) Jeffreys (1942)	-4.1	0	-2.1	0	-.66	0	-.24	33.3								
†(22) Heiskanen (1928)	-6.34	0														
†(23) Heiskanen (1924)	-9.0	+18.0														
†(24) Helmert (1915)	-6.0	-17.0														

*The J_{22} and λ_{22} reported in this table except in one or two instances, have been converted from the original author's set of gravity coefficients of which there are all too many forms in the literature. The blanks indicate the author did not consider that particular tesseral harmonic in fitting an earth potential to the observed data.

†Gravimetric or astro-geodetic tesseral geoids. All other geoid's are either pure satellite geoids or use all three kinds of gravity observations.

		COMMENTS
(17), (20), (22), (23), (24)	Heiskanen and Meinesz: 1958, The Earth and Its Gravity Field (McGraw Hill, N.Y., p. 79)	
(16)	Jeffreys, H: 1959, The Earth (Camb. Univ. Press, N.Y., 4th Ed. Ch. IV and V)	
(18)	Zongolovitch, D: 1957, Bull. Inst. Theoret. Astron. 6,505	
(15)	Kaula W. M: 1959, J. Geophys. Research 64, 2401	
(19)	Subbotin, M. F.: 1959, Course in Celestial Mechanics III (Gostehizdat, Moscow; p. 278)	
(12)	Izsak, I. G: 1961, From the Astronomical Journal 66, #5, 1961 (June) p. 226-229	Uses 2 satellites of medium inclination
(8)	Newton, R. R: 1962, Paper Presented at the Symposium on the Use of Artificial Satellites for Geodesy, April 26-28, 1962, U.S. Naval Observatory, Wash. D.C., (In Press)	
(13)	Kaula, W. M.: 1961, In: H. C. Van De Hulst, C. and De Jager and A. F. Moore, ed., Space Research II; pp. 360-372, North Holland Publishing Co., Amsterdam	
(1), (5)	In: "Non Zonal Harmonic Coefficients of the Geopotential from Satellite Doppler Data," W. H. Guier and R. R. Newton, Johns Hopkins Univ. APL-TG-520, Nov. 1963	
(6)	Kaula, W. M.: "Tesseral Harmonics of the Gravitational Field and Datum Shifts Derived from Camera Observations of Satellites:" Journal of Geophysical Research, Vol. 68 #2, Jan. 15, 1963	
(4)	Kaula, W. M.: "Improved Geodetic Results from Camera Observations of Satellites" (NASA-GSFC) Paper in Press for the Journal of Geophysical Research - May 1963)	
(3)	Izsak, I. G: "Tesseral Harmonics in the Geopotential:" (Nature; July 13, 1963; pp. 137-139	Uses 5 satellites, 1 of very high inclination: with Kaula, probably the most accurate satellite tesseral geoid to high order (through 1963)
(9)	Newton, R. R.: "Ellipticity of the Earth's Equator Deduced from the Motion of Transit 4A" (Journal of Geophysical Research; Vol. 67 #1, Jan. 1962	
(14)	In: "Passive Dynamics in Space Flight" A Bureau of Naval Weapons Paper by J. D. Nicolaides and M. M. Macomber - 1962	
(7)	Kozai, Y. (Oct. 1962): Private Communication to the Author	
(10)	Kozai, Y. (June 1961): "Tesseral Harmonics of the Geopotential of the Earth as Derived from Satellite Motions" (The Astronomical Journal, 66, #7; Sept. 1961	Uses 2 satellites of medium inclination
(2)	Kaula, W. M. (Sept. 1963): "Improved Geodetic Results from Camera Observations of Satellites" (In: The Journal of Geophysical Research; Vol. 68, #18, Sept. 1963)	Uses 5 satellites, of medium inclination
(11)	Kaula, W. M. (June 1961): "A Geoid and World Geodetic System Based on a Combination of Gravimetric, Astro-geodetic and Satellite Data" (Journal of Geophysical Research: Vol. 66, #6, p. 1807)	Probably the most comprehensive "Combined Geoid" to date
(21)	Jeffreys, H. (1942): (In-Monthly Notices of the Royal Astronomical Society, Geophys. Supplement, Vol. 5, 55)	

Table B-2

Comparison of Longitudinal Perturbation Forces on a 24-Hour Satellite, From Five Tesseral Geoids.

	Full Field Longitude Acceleration [Units of 10^{-7} g_s*]	Ratio of Triaxial (J_{22}) Longitude Acceleration to Full Field Longitude Acceleration (λ = -54.75°)
Zhongolovitch (1957)	7.71	1.06
Kozai (1962)	1.08	1.28
Izsak (July 1963)	1.27	1.19
Kaula (Sept. 1963)	1.77	1.11
Wagner (this reduction: March 1964)	2.21	?

*g_s is the radial acceleration of earth gravity at the "synchronous" altitude (g_s = 0.735 ft/sec^2).

Judging from the consistency of the acceleration ratios among these investigators, the "actual" value of J_{22} (separated from higher order gravity effects) is probably somewhat higher than the -1.7×10^{-6} reported herein. All the geodesists reporting in Table B-2 agree that the next most influential earth tesseral at "synchronous" altitudes over most of the equator is J_{33}.

Appendix C

EXPRESSIONS FOR THE INCLINATION FACTOR

Equation (25) gives the inclination factor in the drift causing tangential perturbation (due to equatorial ellipticity) on a 24-hour satellite with a near-circular orbit, as

$$F(i) = \cos(i) + \frac{\Delta\lambda\,(\max)\,\sin^2(i)}{2} \tag{C-1}$$

$\Delta\lambda$(max.) is the absolute value of the maximum longitude excursion of the figure-8 ground track of the 24-hour satellite (with a near-circular orbit) from the geographic longitude of the nodes.

From (18), this longitude excursion function is

$$\Delta\lambda = \lambda - \lambda_0 = \tan^{-1}\left[\cos(i)\tan\theta\right] - \theta \tag{C-2}$$

Differentiating (C-2) with respect to the argument angle θ, the minimax excursion arguments are found from

$$\frac{d(\Delta\lambda)}{d\theta} = 0 = \frac{\cos(i)\sec^2\theta}{1+\cos^2(i)\tan^2\theta} - 1 \cdot \tag{C-3}$$

Solving (C-3) for $\sin\theta$ at $\Delta\lambda$(minimax),

$$\sin\theta_{\Delta\lambda(\text{minimax})} = \left[\cos(i)+1\right]^{-1/2}, \quad \text{from which}$$

$$\tan\theta_{\Delta\lambda(\text{minimax})} = \sec(i), \tag{C-4}$$

(C-4) in (C-2) gives

$$\Delta\lambda(\text{minimax}) = \tan^{-1}\left[\cos(i)\sec(i)\right] - \tan^{-1}\sec(i).$$

Thus, since only the absolute value of $\Delta\lambda$(minimax) is required,

$$\Delta\lambda(\max) = \tan^{-1}\left[\sec(i)\right] - 45^\circ, \tag{C-5}$$

where the $\tan^{-1}$ is to be taken in the first quadrant. For example: for $i = 30°$, (C-5) evaluates the maximum excursion as

$$\Delta\lambda(\max) = 49.1° - 45° = 4.1° .$$

The nodal argument angle at this maximum longitude excursion is

$$\theta\left[\text{at } \Delta\lambda(\max)\right] = \pm 49.1° \text{ from the nodes.}$$

The assumption in (20) that the excursion in longitude from the ascending node could be approximated by

$$\Delta\lambda - \Delta\lambda(\max) \sin 2\theta ,$$

predicts the maximum excursion argument as

$$\theta\left[\text{at } \Delta\lambda(\max)\right] = \pm 45° \text{ from the nodes.}$$

This discrepancy in the assumed longitude excursion function is not serious until $i > 45°$, as simulated trajectories with variable inclination have borne out.

(C-5) can be written as

$$\Delta\lambda(\max) + 45° = \tan^{-1}\left[\sec(i)\right] , \text{ from which}$$

$$\tan\left[\Delta\lambda(\max) + 45°\right] = \sec(i) \pm \frac{1 + \Delta\lambda(\max)}{1 - \Delta\lambda(\max)} , \qquad \text{(C-6)}$$

for $i < 45°$. Solving (C-6) for $\Delta\lambda$ (max),

$$\Delta\lambda(\max) = \frac{1 - \cos(i)}{1 + \cos(i)} , \qquad \text{(C-7)}$$

approximately.

Thus the inclination factor becomes approximately

$$F(i) = \cos(i) + \frac{\sin^2(i)\left[1 - \cos(i)\right]}{2\left[1 + \cos(i)\right]}$$

$$= \cos(i) + \frac{\left[1 - \cos(i)\right]^2}{2} = \frac{2\cos(i) + 1 - 2\cos(i) + \cos^2(i)}{2}$$

$$= \frac{\cos^2(i) + 1}{2} \qquad \text{(C-8)}$$

For example: For $i = 30°$,

$$F(i)_{\text{from (C-1)}} = .86603 + 4.1/8 \times 57.3 = .8750$$

$$F(i)_{\text{from (C-8)}} = .8750 .$$

The agreement of $F(i)$ from forms (C-1) or (C-8) is good to the third decimal place as long as the inclination is less than 45 degrees. At inclinations higher than 45 degrees, however, the drift theory following (20) begins to break down because $\Delta\lambda$(max) is no longer a small angle.

Appendix D

DERIVATION OF THE EXACT ELLIPTIC INTEGRAL OF DRIFT MOTION FOR A 24-HOUR SATELLITE WITH A NEAR-CIRCULAR ORBIT: COMPARISON OF THE EXACT SOLUTION WITH THE APPROXIMATE SOLUTIONS FOR PERIODS VERY CLOSE TO SYNCHRONOUS

The differential equation (33) of 24-hour satellite drift is analogous to the equation describing the large-angle oscillations of a mathematical pendulum (see Reference 11), as in Figure D-1.

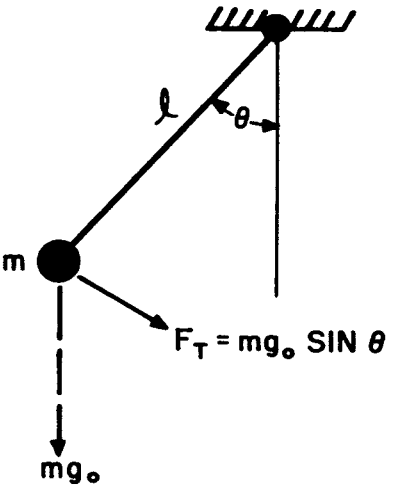

Figure D-1—Configuration of a "mathematical pendulum."

The equation of angular motion of the mass m under the constant gravity force mg_0 is

$$F_T = mg_0 \sin\theta = m(\dot{l}\dot{\theta}) = ml\ddot{\theta} \qquad \text{(D-1)}$$

(D-1) can be rewritten as

$$\ddot{\theta} + (g_0/l) \sin\theta = 0 . \qquad \text{(D-2)}$$

From the theory developed in Reference 11 (pp. 327-335), (D-2) has an integral

$$t \text{ (time from } \theta = 0) = (l/g_0)^{1/2} F(\underline{k}, \phi) , \qquad \text{(D-3)}$$

where $F(\underline{k}, \phi)$ is the elliptic integral of the first kind with argument (or amplitude) $\phi = \sin^{-1}\left[\frac{\sin\theta/2}{\sin\theta\,(\max)/2}\right]$, and modulus $\underline{k} = \sin\theta\,(\max)/2$.

Equation (33):

$$\ddot{\gamma} + A_{22} \sin 2\gamma = 0 ,$$

with maximum libration angle γ_0, can be put in the form of (D-2) by the transformation of the dependent variable

$$\theta = 2\gamma , \qquad \text{(D-4)}$$

with the parameter identification

$$g_0/l = 2A_{22} \quad . \tag{D-4A}$$

(D-4) implies the identification

$$\underline{k} = \sin\gamma_0 , \qquad \underline{\phi} = \sin^{-1}\left[\sin\gamma/\sin\gamma_0\right] \quad . \tag{D-4B}$$

The pendulum solution (D-3), under the transformation (D-4) and identifications (D-4A) and (D-4B) becomes

$$t \text{ (time of drift libration from } \gamma = 0)$$

$$= \left(1/2A_{22}\right)^{1/2} F\left(\sin\gamma_0 \ , \ \left[\sin^{-1}\sin\gamma/\sin\gamma_0\right]\right), \tag{D-5}$$

$F(\underline{k}, \underline{\phi})$, in its full integral form, is

$$F = \int_0^{\underline{\phi}} \frac{d\underline{\phi}}{\left(1 - \underline{k}^2 \sin^2\underline{\phi}\right)^{1/2}} \quad , \tag{D-6}$$

(where $\underline{k}^2 = \sin^2\gamma_0$, $\sin^2\underline{\phi} = \sin^2\gamma/\sin^2\gamma_0$) for the drift libration. In particular, when $\underline{\phi} = \pi/2$; then $\gamma = \gamma_0$; $\dot{\gamma}_0 = 0$, and the pendulum-drift libration has completed a quarter-period.

Thus, from (D-5) and (D-6), the full period of the long-term drift libration of the 24-hour satellite ground track about the nearest minor equatorial axis longitude is

$$T(\gamma_0) = \left[8/A_{22}\right]^{1/2} \int_0^{\pi/2} \frac{d\psi}{\left(1 - \sin^2\gamma_0 \sin^2\psi\right)^{1/2}} \quad . \tag{D-7}$$

The adequacy of the Taylor series expansion approximation of the drift motion in the neighborhood of γ_0, given in equation (51), may be tested against the exact drift solution implicit in (D-5). Table D-1 below gives the evaluation of F for arguments within 5° of $\gamma_0 = 60°$, using the integral tables in Reference 12.

Table D-1

Exact and Approximate Drifts of a 24-Hour Satellite from a Stationary Configuration 60° East of the Earth's Minor Equatorial Axis.

$\gamma_0 = 60°$	γ (degrees)	γ' (degrees)	γ'' (degrees)	ϕ (degrees)	F (rad.)	ΔF (rad.)	Δt (days from $\gamma = 60°$)
$A_{22} = 23.2 \times 10^{-6}$ rad/day^2	60.0	60.0	60	90	2.1565	-	-
	59.0	59.003	59.000	81.7967	1.8730	.2835	41.619
	58.0	58.014	58.001	78.3056	1.7564	.4001	58.737
	57.0	57.029	56.999	75.5595	1.6671	.4894	71.846
	56.0	56.051	56.999	73.1938	1.5923	.5642	82.827
	55.0	55.077	54.996	71.0617	1.5265	.6300	92.487

In Table D-1, ΔF is the change in the elliptic integral from the "stationary" configuration at $\gamma = 60°$ or $\phi = 90°$. $\Delta t = (1/2A_{22})^{1/2}\Delta F$. A_{22} was computed from (30A) with the following gravity-earth constants and for the inclination of Syncom II:

$$R_0 = 6378.2 \text{ km}$$

$$a_s = 42166 \text{ km}$$

$$J_{22} = -1.7 \times 10^{-6}$$

$$i = 33°.$$

γ' gives the drift position as calculated from the first righthand term of (51) alone (the $(\Delta t)^2$ term). γ'' gives the drift position as calculated from the first two righthand terms of (51). The "actual" Syncom II drift in mid-August 1963 began, apparently, at a γ_0 between 48° and 58° east of the minor axis. Thus, the 16 orbits chosen for the first drift period all should be well represented by the $(\Delta t)^2$-only theory, within the rms error of the longitude observations. Similar exact calculations for $\gamma_0 = 45°$, 50°, and 55° confirm the adequacy of the $(\Delta t)^2$-only theory to apply to the second drift-period orbits. They also prove the contention in section 5 that, for reasonably small excursions from "synchronism," the convergence of the Taylor series (51) is adequate if additional terms are included only when they become of a certain minimum significance to the total drift.

Appendix E

BASIC ORBIT DATA USED IN THIS REPORT

The Orbit elements for Syncom II in Table E-1 were calculated at the Goddard Space Flight Center from radar and Minitrack observations made during the slow drift periods from mid-August 1963 to February 1964.

As an example of the estimation of the ascending equator crossing nearest to epoch, consider the orbit geometry at epoch (Figure E-1).

6 January 1964 at 17.0 hours Universal Time (orbit 2-5) .

Table E-1

Syncom II Orbital Elements, August 1963 to February 1964.

Orbit #	Epoch (Universal Time) Year-Month-Day-Hour-Min	Semimajor Axis (km)	Eccentricity	Inclination (degrees)	Mean Anomaly (degrees)	Argument of Perigee (degrees)	Right Ascension of the Ascending Node (degrees)
1-1	63-8-22-6-12-14	42164.58	.00018	33.083	24.126	26.285	317.569
1-2	63-8-26-17-0	42164.52	.00016	33.090	190.841	26.099	317.454
1-3	63-8-31-0-0	42166.02	.00018	33.062	296.125	30.073	317.475
1-4	63-9-5-0-0	42166.39	.00012	33.064	333.521	357.756	317.362
1-5	63-9-9-0-0	42166.35	.00015	33.048	326.207	9.077	317.272
1-6	63-9-12-2-0	42166.55	.00015	33.079	3.657	4.697	317.224
1-7	63-9-17-2-0	42166.70	.00018	33.043	12.694	0.581	317.165
1-8	63-9-20-2-0	42167.42	.00018	33.010	359.970	16.282	317.098
1-9	63-9-27-2-0	42167.51	.00022	33.046	38.922	344.162	316.996
1-10	63-10-1-2-0	42168.88	.00024	33.039	26.615	0.433	316.944
1-11	63-10-8-2-0	42169.14	.00020	33.013	42.889	350.866	316.780
1-12	63-10-14-2-0	42169.78	.00028	32.982	36.727	2.673	316.813
1-13	63-10-22-2-0	42171.51	.00026	32.993	62.833	344.246	316.603
1-14	63-10-30-0-0	42171.09	.00028	32.948	29.865	354.548	316.570
1-15	63-11-6-0-0	42172.15	.00025	32.952	36.699	354.313	316.328
1-16	63-11-12-0-0	42172.51	.00031	32.920	108.239	3.425	316.308
2-1	63-11-28-1-0	42165.89	.00005	32.920	222.170	203.901	315.976
2-2	63-12-4-0-0	42167.20	.00009	32.892	39.435	17.564	315.919
2-3	63-12-10-0-0	42167.18	.00010	32.881	51.942	10.958	315.877
2-4	63-12-16-17-0	42168.17	.00007	32.872	300.000	24.505	315.735
2-5	64-1-6-17-0	42168.01	.00013	32.867	332.997	11.625	315.544
2-6	64-1-9-6-0	42169.90	.00015	32.857	165.031	16.992	315.469
2-7	64-1-20-0-0	42171.43	.00012	32.826	29.098	28.842	315.300
2-8	64-1-29-20-0	42171.91	.00019	32.859	37.956	13.171	315.212
2-9	64-2-5-16-0	42172.89	.00019	32.800	321.168	36.275	315.075
2-10	64-2-10-19-0	42173.31	.00014	32.833	32.517	14.553	314.982
2-11	64-2-17-0-0	42174.89	.00019	32.762	347.774	35.551	314.883

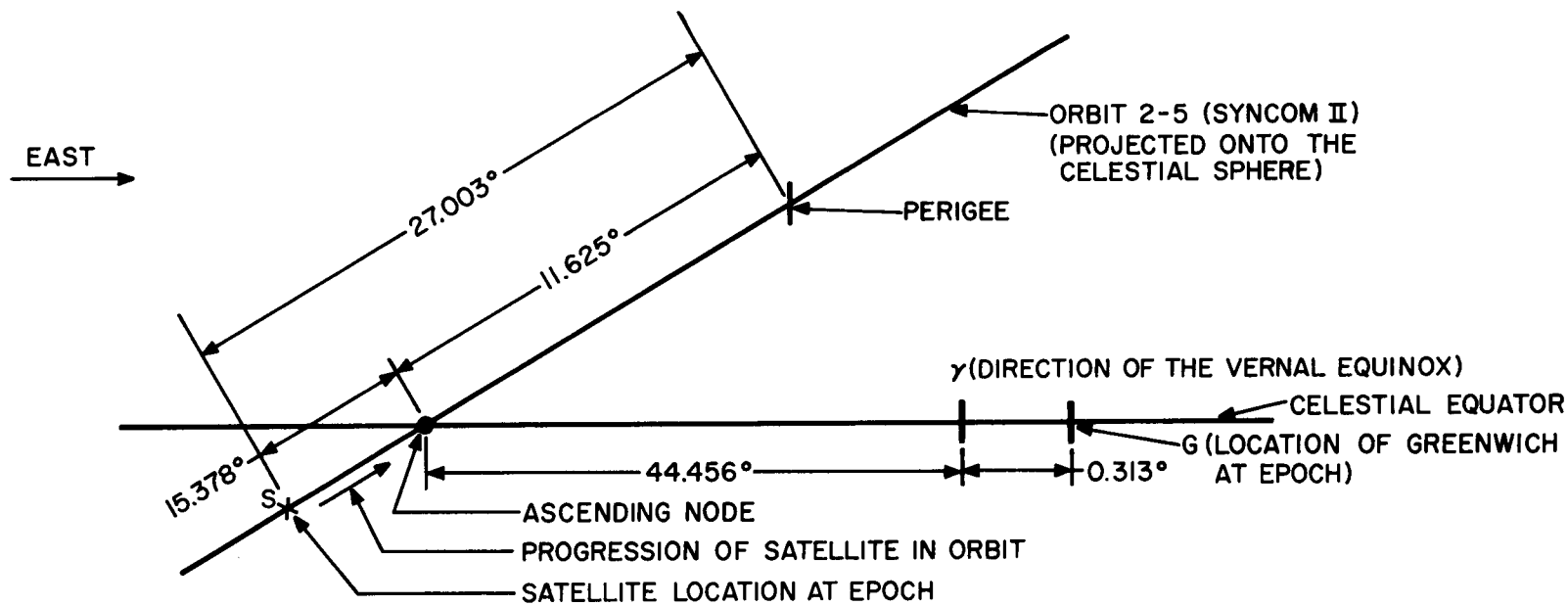

Figure E-1—A portion of the celestial sphere at the epoch of orbit 2-5

On 6.0 January 1964, the hour angle of the vernal equinox Λ *west* of Greenwich (expressed in hours, with 24 hours = 360°) was

6 hrs 58 minutes 27.484 seconds (from the Nautical Almanac)

On 7.0 January 1964, the hour angle of Λ was

7 hrs 2 min 24.036 sec.

Interpolating, the hour angle of Λ on 6 January at 17 hours Universal Time was

0 hours 1 minute 15.042 seconds, or
0.313 degrees west of Greenwich .

In Figure E-1, the orbit angle 27.003° is taken directly as 360° - the mean anomaly, because the orbit is nearly circular. The reported period for this orbit was

$$T_p = 1436.21696 \text{ minutes} .$$

The earth's sidereal rotation period is taken to be

$$T_{earth} = 1436.06817 \text{ minutes} .$$

Thus, if the satellite is assumed to traverse orbit 2-5 at a nearly uniform rate, it will reach the celestial equator at a time when the Greenwich meridian has proceeded eastward from the epoch

$$15.378 \times 1436.21696/1436.06817 = 15.380° .$$

Thus, the estimated geographic longitude of the ascending equator crossing nearest to the epoch of orbit 2-5 is

$$\text{Ascending equator crossing longitude} = -(44.456 + 0.313 + 15.380)$$
$$= -60.149° .$$

The estimated time of this crossing is

$$15.380°/15°/\text{hr.} = 1.025 \text{ hours after the epoch} .$$

The crossing time (Table 1) is thus estimated to be at

6.751 January 1964 (18.025/24 + 6.0, January 1964) .

Appendix F

CALCULATION OF THE RADIATION PRESSURE ON SYNCOM II

Consider a flat-plate element ΔA, of the surface of Syncom II, whose normal $\bar{n}$ is at angle θ with respect to the sun's rays (Figure F-1). The sun's radiant energy can be thought of as being made up of a stream of material particles such as dm, moving at the speed of light c. If the energy of each particle is dE, then from Einstein's classical energy-mass equivalence statement,

$$dm = dE/c^2 \ . \qquad \text{(F-1)}$$

Upon striking the surface, the incident radiation may:

- Reflect completely off the surface at an equal "reflection" angle, undegraded in energy
- Be absorbed into the body of the plate as thermal energy and partially reradiated in all directions from the surface at a reduced flux, depending on the surface and on the thermal properties of the plate and body of the spacecraft
- Be partially "reflected" and absorbed and reradiated, depending on the surface properties of the plate

An estimate of the radiation pressure on Syncom II will be calculated assuming complete light absorption with no reradiation. This is not the most conservative condition but will serve to show the order of magnitude of the effect.

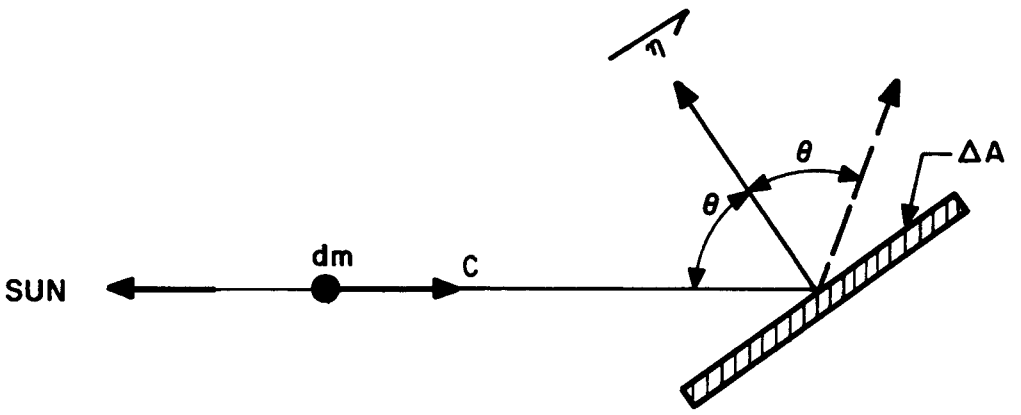

Figure F-1—Flat plate ΔA of satellite surface, with normal $\overrightarrow{\eta}$ at angle θ with respect to sun's rays.

Light-particle dm has c dm momentum in the direction of the sun's rays before striking the plate element ΔA. Thus (c) dm momentum is transferred to the plate with each light-particle collision. From Newton's second law, the impulse transferred to the plate in the time of action dt, of dm alone, is;

$$\int_0^{dt} (dF)_{dm}\, dt = (c)\, dm , \tag{F-2}$$

dF acts on the plate element in the direction of the sun's rays. Assume that the discontinuous collision processes of (F-2) are so frequent as to amount to a smooth transfer of momentum between the stream of light particles and the plate; dt can then be replaced by Δt, a small but finite time interval; $(dF)_{dm}$ by ΔF, a smooth, constant small reactive force on the plate element ΔA; and dm can be replaced by Δm, a small but finite light particle mass impinging on the plate surface ΔA in Δt time. (F-2) then becomes

$$\Delta F(\text{radiation force})\ \Delta t = (c)\Delta m, \text{ or}$$

$$\Delta F(\text{radiation force}) = (c)\frac{\Delta m}{\Delta t} . \tag{F-3}$$

By the mass-energy equivalence relation (F-1) written for the finite small elements involved in the continuous momentum transfer,

$$\Delta m = \Delta E/c^2 , \tag{F-4}$$

where ΔE is the energy flux falling on plate element ΔA in Δt time. Clearly,

$$\Delta E = \rho\, \Delta A \cos\theta\, (\Delta t) , \tag{F-5}$$

where ρ is the sun's energy flux in units of energy/time-area, and $\Delta A \cos\theta$ is the projected area of the element in the direction of the sun's rays. Combining (F-3), (F-4) and (F-5);

$$\Delta F/\Delta A_p = \text{projected area-radiation pressure in the direction of the sun's rays} = p_s = \frac{\rho}{c} , \tag{F-6}$$

($\Delta A_p = \Delta A \cos\theta$ = projected area of the plate element in the direction of the sun's rays.)

The value of ρ outside the earth's atmosphere is estimated to be (see Reference 9)

$$\rho = 95.5 \text{ ft-pounds/ft}^2\text{-sec.}$$

$$c = 9.835 \times 10^8 \text{ ft./sec.}$$

(F-6) thus becomes;

$$P_s \text{ (projected area-solar pressure against a fully absorbing surface in the direction of the sun's rays)} = .9725 \times 10^{-7} \text{ pounds/ft.}^2 \qquad \text{(F-7)}$$

Figure F-2 shows the configuration of Syncom II with respect to the sun during the drift. For the cylindrical configuration in Figure F-2, from (F-7);

$$F(\text{absorb-total}) = F(\text{absorb-body}) + F(\text{absorb-end}) = .9725 \times 10^{-7} \left(HD \cos\theta + \pi D^2 \sin\theta/4\right) \text{(F-8)}$$

The weight of Syncom II in the 24-hour orbit (including the apogee motor) is about 75 pounds. Other parameters are:

$H = 15''$

$D = 28''$

$\theta = 21°$ (in late August 1963) .

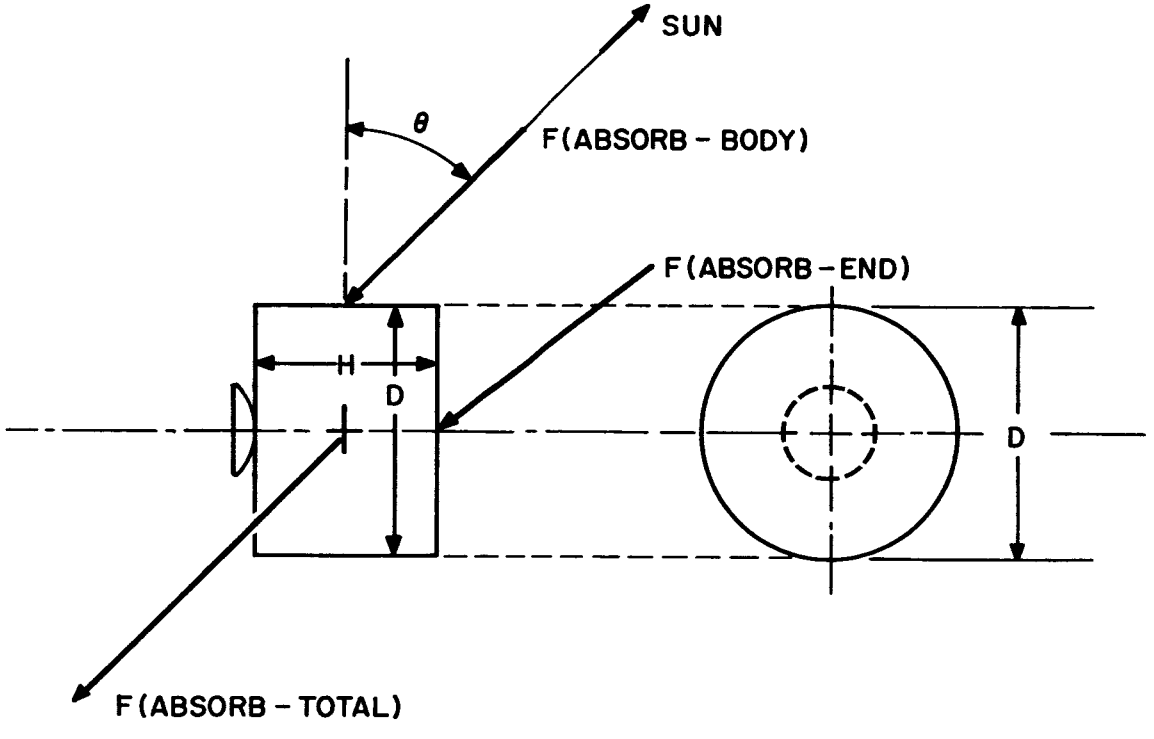

Figure F-2—Configuration of Syncom II with respect to the sun during drift.

Thus, $HD\cos\theta + \pi D^2 \sin\theta/4 = 613\ \text{in}^2 = 4.25\ \text{ft}^2$; from (F-8),

$$F\,(\text{radiation force with total absorption}) = 4.13 \times 10^{-7}\ \text{pounds}.$$

The mean solar gravity force on Syncom II in orbit is given as

$$F\,(\text{solar gravity}) \doteq \frac{\mu_s \times 75/32.15}{(1\,\text{A.U.})^2},$$

where 1 astronomical unit (A.U. = the earth's mean distance from the sun) $\doteq$ 92,900,000 miles $= 4.9 \times 10^{11}$ ft.

$$\mu_s = 333{,}000\,\mu_E = 333{,}000 \times 1.40765 \times 10^{16}\ \text{ft}^3/\text{sec}^2 = 4.18 \times 10^{21}\ \text{ft}^3/\text{sec}^2.$$

Therefore

$$F\,(\text{solar gravity on Syncom II}) \doteq \frac{4.18 \times 10^{21} \times 75}{(4.9)^2 \times 10^{22} \times 32.15} = 4.07 \times 10^{-2}\ \text{pounds}.$$

It is evident that solar radiation pressure on Syncom II causes perturbations which are insignificant compared to solar gravity perturbations.